Structure-Reactivity-Property Relationships in Covalent Adaptable Networks

Vivian Zhang,[‡] Boyeong Kang,[‡] Joseph V. Accardo,[‡] Julia A. Kalow*

Department of Chemistry, Northwestern University, 2145 Sheridan Road, Evanston, IL 60208, United States

ABSTRACT: Polymer networks built out of dynamic covalent bonds offer the potential to translate the control and tunability of chemical reactions to macroscopic physical properties. Under conditions at which these reactions occur, the topology of covalent adaptable networks (CANs) can rearrange, meaning that they can flow, self-heal, be remolded, and respond to stimuli. Materials with these properties are necessary to fields ranging from sustainability to tissue engineering; in these contexts, however, the conditions and timescale of network rearrangement must be compatible with the intended use. The mechanical properties of CANs are based on the thermodynamics and kinetics of their constituent bonds. Therefore, strategies are needed that connect the molecular and macroscopic worlds. In this Perspective, we analyze structure-reactivity-property relationships for several classes of CANs, illustrating both general design principles and the predictive potential of linear free energy relationships (LFERs) applied to CANs. We discuss opportunities in the field to develop quantitative structure-reactivity-property relationships and open challenges.

1. INTRODUCTION

Over a century of polymer science has enabled materials to be programmed with unprecedented control. The addition of chemical (covalent) linkages between polymers, or crosslinking, leads to the formation of polymer networks with distinct properties. During crosslinking, individual polymer strands with discrete molecular weights are jointed into a network structure of effectively infinite molecular weight, where the motion of polymer segments becomes

limited by the introduction of permanent multifunctional junctions. The discovery of synthetically-crosslinked polymers that rivaled natural materials has enormous historical significance and led to the ubiquity of polymer networks in modern society, a notable example being the synthetic vulcanization of harvested latex with sulfur to produce natural rubber (**Figure 1a**). Crosslinking is not limited to synthetic networks. Nature's crosslinking of fibrillar collagens is essential for proper development of connective tissues, and mutations affecting the enzymes responsible (e.g. lysyl oxidase) lead to impaired tissue integrity (**Figure 1b**).

Figure 1. Crosslinking polymer strands produces polymer networks in (a) synthetic (b) and natural systems. Micrograph reprinted with permission under a Creative Commons Attribution (CC BY4.0) License from ref. ³. Copyright David Gregory and Debbie Marshall.

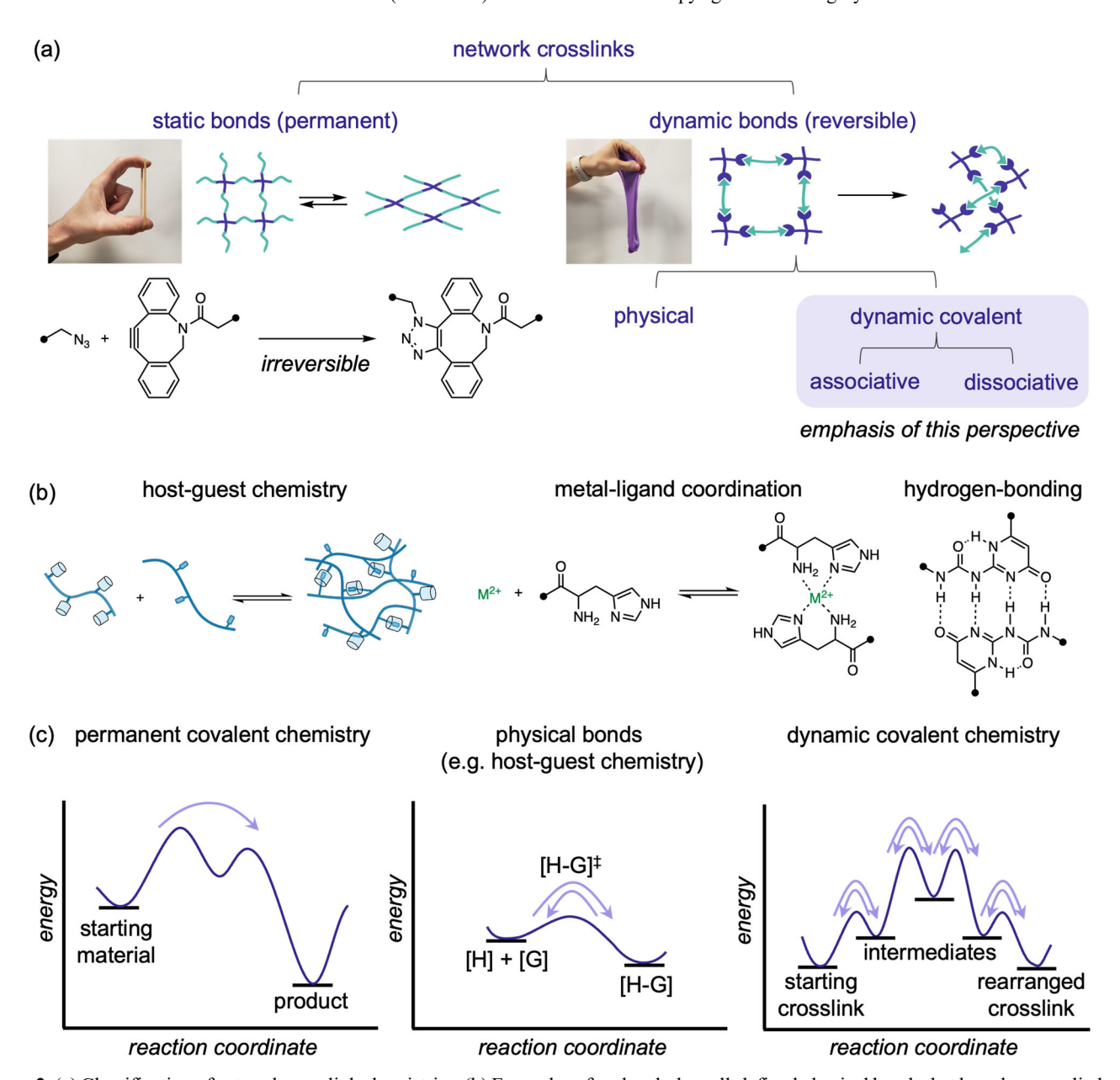


Figure 2. (a) Classification of network crosslink chemistries. (b) Examples of molecularly well-defined physical bonds that have been applied to dynamic networks. (c) Representative mock reaction landscapes of crosslink chemistries. Permanent covalent chemistries undergo irreversible single-step or multistep mechanisms. Physical bonds are reversible, often through low-barrier, single-step mechanisms. Dynamic covalent chemistries are reversible, and many undergo multi-step exchange mechanisms. A representative landscape for Lewis acid-catalyzed transesterification is depicted with steps corresponding to Lewis acid activation, nucleophilic attack, elimination, and Lewis acid decomplexation.

Experimental and theoretical research has demonstrated that the physical properties of polymer networks are intimately linked to their composition and topology. Networks comprised of permanent covalent crosslinks are strong and durable, but the irreversible nature of their crosslinking renders them unable to rearrange molecularly. These materials cannot be repaired or remolded because their topologies are static, and they cannot adapt to applied forces (Figure 2a). Introducing crosslinks based on dynamic interactions has expanded the functions of polymer networks. These networks can rearrange over time, leading to *viscoelasticity*, characterized by both solid-like and

fluid-like properties. Viscoelasticity enables behaviors such as self-healing, moldability, injectability, and stimuli-responsiveness. There are a wide variety of dynamic crosslinks with a broad range of binding strengths, temperature dependences, and exchange timescales, rendering them suitable for many potential applications.⁵ The focus of this Perspective is networks based on dynamic covalent bonds, which have been coined covalent adaptable networks (CANs)⁶ or dynamic covalent polymer networks (DCPNs).⁷

Structure-reactivity-property relationships relate crosslink structure to its reactivity and thus to the mechanical properties of the corresponding network. Ideally, these relationships could be applied predictively to engineer a network to target stiffness, temperature dependence, and timescale of rearrangement that match the intended application. For example, a plastic with improved recyclability should exhibit flow at elevated temperatures but undergo minimal rearrangement at room temperature. Similarly, a dynamic hydrogel for biomimetic cell culture should match the mechanics of the native tissue of interest at 37 °C and cannot employ cytotoxic catalysts.

In this Perspective, we illustrate how the same physical organic strategies that are used to understand and manipulate small-molecule reactions can be applied to polymer networks built upon dynamic covalent reactions. We contend that quantitative structure-reactivity-property relationships for dynamic networks will allow researchers to predictably design materials with targeted mechanical properties. However, we also discuss the complicating factors inherent to polymer networks that occlude straightforward analysis of these relationships. The examples we highlight will range from solvated, soft gels to stiff thermosets, with the common factor being dynamic covalent crosslinks. For researchers seeking to apply CANs in specific contexts, we hope this Perspective serves as a user's guide to selecting and tuning dynamic crosslinks. For synthetic chemists

incorporating new dynamic chemistries into CANs, we discuss how molecular reactivity translates to network properties and how to characterize these materials. For existing experts in this field, we provide recommendations about how small-molecule and polymer systems can be designed and analyzed to best yield quantitative relationships. Finally, for theorists and measurement scientists, we describe critical gaps in knowledge and tools and how their contributions could advance this field.

1.1 TYPES OF DYNAMIC BONDS

Non-covalent interactions such as hydrogen bonding, π - π stacking, ionic interactions, protein-protein interactions, metalligand interactions, and host-guest chemistry, among others, are the foundation for *physical* bonds (**Figure 2b**). These non-covalent interactions are readily tuned by modifications such as changing the guest molecule in a host-guest complex or the metal ion in a metal-ligand complex. Network properties are controlled by selecting binding partners with desired binding strengths and association and dissociation kinetics. These interactions have enabled seminal developments in structure-reactivity relationships in polymer networks. Supramolecular networks have been reviewed elsewhere. Supramolecular

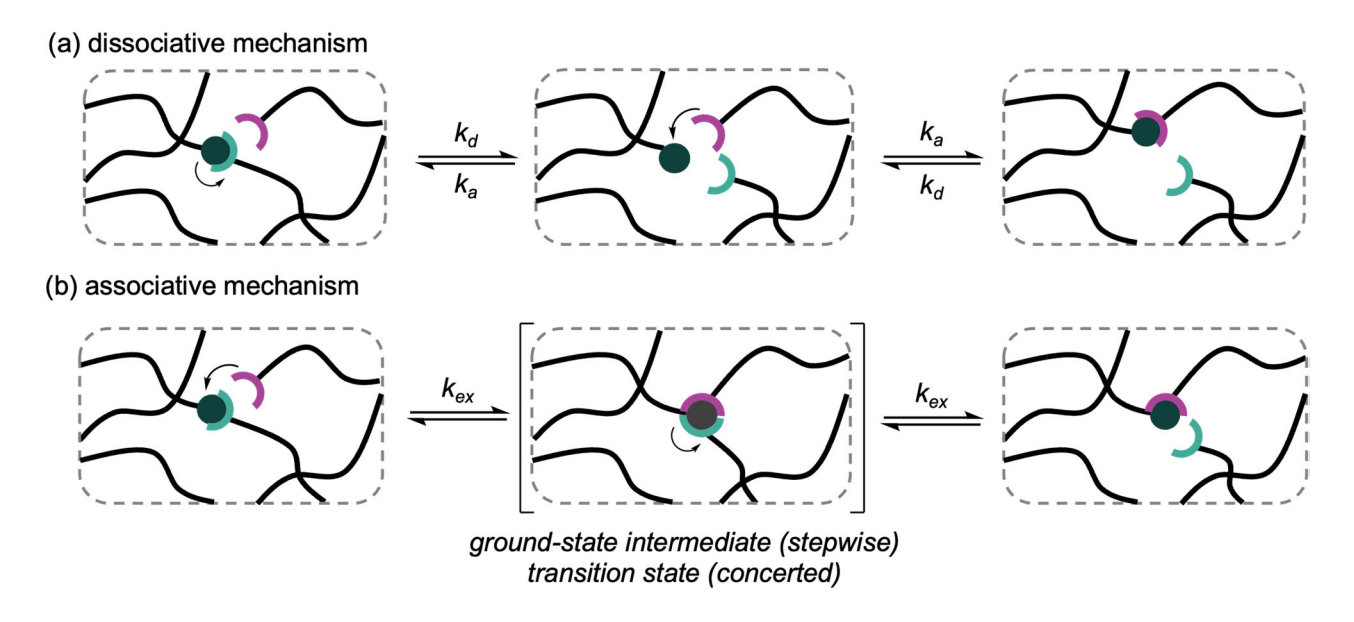


Figure 3. Schematic representation of (a) dissociative and (b) associative crosslinker exchange.

Dynamic covalent bonds couple the exchangeable nature of physical crosslinks with the strength and directionality of covalent bonds. ¹⁹ Both dynamic covalent and physical bonds are sensitive to changes in structure and environmental factors including pH, temperature, and concentration, conferring the potential for stimuli-responsiveness. The use of light as an external stimulus to alter the reactivity of dynamic covalent bonds is of particular interest to our group (Section 3.3). While both types of bonds are reversible, exchange with dynamic covalent bonds is often mechanistically more complex, occurring through multi-step processes with one or more intermediates (**Figure 2c**). For comprehensive lists of dynamic bonds and data that demonstrate the range of reactivity achievable by dynamic covalent chemistry, we direct readers to reviews and perspectives by Sumerlin, Konkolewicz, Xie, Bowman, ¹⁸ and Dichtel. ^{20–24}

1.2 EXCHANGE MECHANISMS

Dynamic exchange occurs through associative or dissociative mechanisms. *Dissociative* dynamic crosslinks first break apart before rebonding with the original or a different unoccupied partner (**Figure 3a**). In comparison, crosslinks that exchange through an *associative* mechanism undergo displacement of one partner for another, often through an addition-elimination sequence (**Figure 3b**).⁶ Dry networks that rearrange through associative mechanisms have been termed vitrimers.^{25–27} Because both classes of CANs are based on chemical reactions, they share many attributes, such as Arrhenius behavior, and both mechanisms offer substantial molecular tunability.²³ A key distinction is that dissociative networks tend to exhibit a gel–sol transition at temperatures where debonding becomes entropically favorable, while the crosslink density of vitrimers is con-

served and the stiffness should increase as a function of temperature due to entropic elasticity. ^{5,28} Furthermore, associative networks are considered more solvent-resistant than dissociative ones, although dissolution through an associative mechanism is possible. ^{29–32} In practice, holistic considerations about the target application and use conditions (e.g. dry network vs. gel, temperature, pH, chemical compatibility) should inform the type of dynamic chemistry that is selected.

When multiple mechanisms are available, the environment and crosslink structure will determine the dominant pathway and must be carefully considered.³³ For example, boronic esters and imines³⁴ exchange through different mechanisms depending on the presence or absence of aqueous solvent (**Figure 4a**). In aqueous or humid environments, these bonds exchange primarily through a dissociative mechanism consisting of hydrolysis and condensation. Moreover, the speciation of boronic acids and esters between more-reactive trigonal and less-reactive tetrahedral forms depends on solution pH and the structure of the boronic acid and diol.^{35–38} In dry networks, boronic esters

exchange associatively through either transesterification with free diol. In the absence of excess diol, a metathesis mechanism has been proposed.³⁹ Mechanistic ambiguity is a common challenge in CANs due to the many factors that can influence reactivity and obstacles to direct mechanistic studies in the material. In a triazolium CAN developed by Drockenmuller, the originally proposed concerted transalkylation mechanism was ultimately revealed to occur through counterion-mediated dissociative exchange (Figure 4b). 40,41 Using this insight, Winne and Du Prez developed an analogous ionic vitrimer based on sulfonium-thioether transalkylation, using a non-nucleophilic arylsulfonate counterion to promote concerted exchange.⁴² Konkolewicz demonstrated that the anilinium CAN exhibited a high degree of association within the temperature range studied, with a virtually constant crosslinking density despite a dissociative mechanism. 43 As the stress relaxation measurements took place below the gel temperature at which entropic factors favor substantial debonding, minor elasticity losses that are hypothesized to arise from heating a dissociative network were not detected.

(a) dissociative boronic ester condensation in aqueous environment

associative boronic ester transesterification in dry network (excess diol)

associative boronic ester metathesis in dry network (no excess diol)

(b) proposed mechanism: concerted $S_N 2$ transalkylation

$$\begin{array}{c} X^{\ominus} \\ \\ N^{\bullet} \\ N^{\bullet} \end{array} \longrightarrow \begin{bmatrix} X^{\ominus} \\ \\ N^{\bullet} \\ N^{\bullet} \\ N^{\bullet} \end{bmatrix}^{\ddagger} \longrightarrow \begin{bmatrix} X^{\ominus} \\ \\ N^{\bullet} \\ N^{\bullet} \\ N^{\bullet} \end{bmatrix}^{\bullet}$$

actual mechanism: counterion-mediated dissociative exchange

Figure 4. Examples of dynamic bonds with multiple exchange mechanisms. (a) Boronic esters exchange through a dissociative mechanism in aqueous environments and associative transesterification or metathesis (proposed) in dry networks. (b) 1,2,3-Triazolium CANs exchange through a dissociative counterion-mediated stepwise rearrangement, not the originally proposed associative transalkylation.

The upside of this complexity is tunability. Across diverse dynamic covalent bonds, certain unifying principles can help users select, analyze, and tune the appropriate system for a given study or application. In Section 2, we discuss theories that have been developed to describe the relationships between crosslink reactivity and network mechanics in dynamic networks. We also review how relevant properties are commonly probed in both small molecules and materials. In Section 3, we showcase examples of systematic structure-reactivity-property studies from the literature including electronic and steric variation, internal catalysis, and photoswitchable reactivity. In Section 4, we outline recommendations and our outlook for the field.

2. THEORIES AND ESTABLISHED RELATIONSHIPS

Relationships between network viscoelasticity and crosslink reactivity and stability that have been established over the last several decades were developed based on systems with physical (non-covalent) crosslinks. 44-50,9,10 Here, we seek to describe these theories in relation to CANs at a level accessible to synthetic chemists. For a more thorough discussion of the polymer physics of dynamic networks, the reader is directed to a review by Webber and Tibbitt.⁵

There has been a recent push to develop theories for CANs, with vitrimers attracting significant attention. 51-56 The study of

CANs poses additional challenges because unlike the singlestep dissociative mechanisms exhibited by many supramolecular crosslinks, dynamic covalent bonds may exchange through multi-step mechanisms, each step with its own associated energies and barriers. Experimental analysis is limited to the ratelimiting step, which can vary as the crosslink structure or environment change. Nevertheless, CANs can still be systematically studied using the principles established for physical networks, yielding useful insights to tune network properties.

2.1 CROSSLINK FORMATION AND NETWORK STIFFNESS

Networks may be formed by combining multifunctional small molecules or crosslinking grafted or star prepolymers (**Figure 5a**). Here, we refer to the multifunctional branch points that provide the network structure as "junctions", while the chemical bond used to join monomers or prepolymers into the network is the "crosslink". The junctions are connected by polymer strands. For multifunctional dynamic covalent crosslinks like borates (B(OR)₃), and for bifunctional small molecules that join grafted polymers, the crosslink is also a dynamic junction with functionality 3 and 4, respectively. However, when star polymers are crosslinked by a dynamic bond between two reactive end groups, the junction is instead the non-dynamic central multifunctional core and the crosslink is part of the strand.

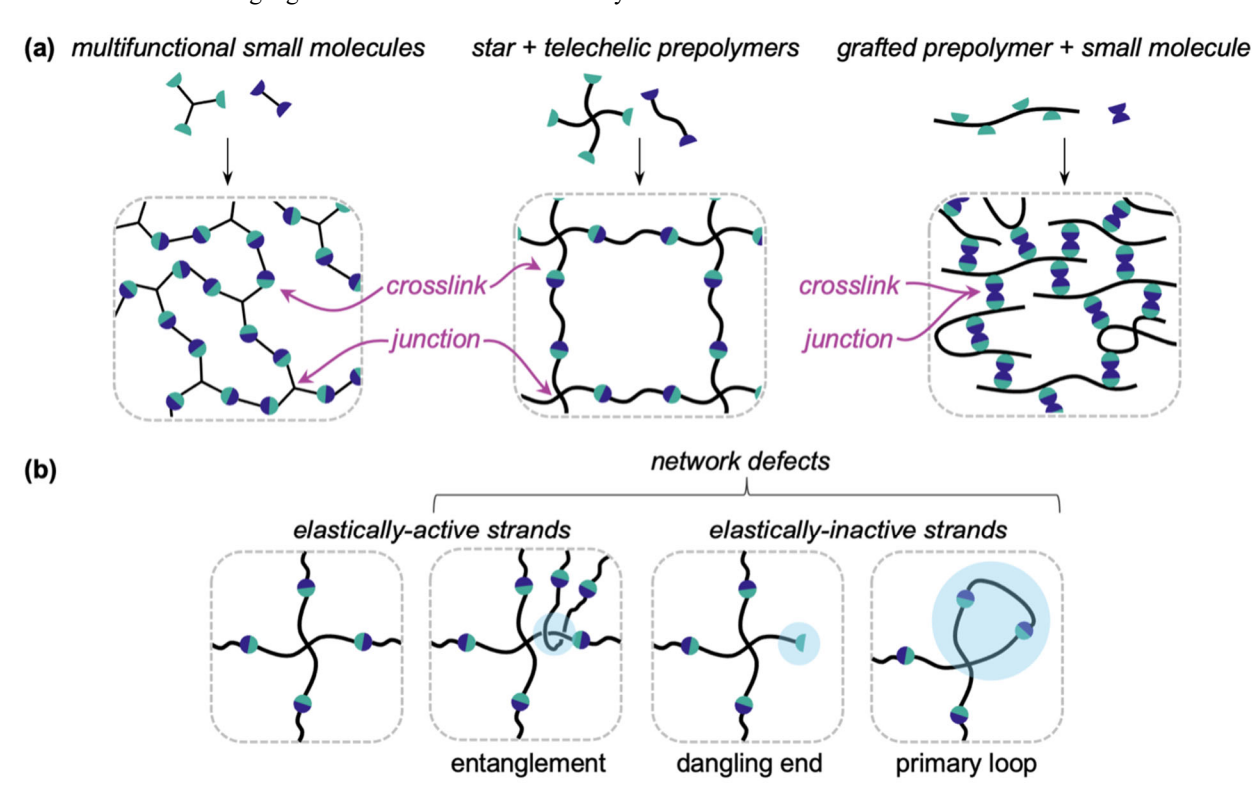


Figure 5. (a) Representative strategies to form networks. (b) Illustration of elastically active and inactive strands obtained by reaction between 4-arm and telechelic prepolymers in real networks.

When force is applied to a network (stress = force/area) and it undergoes deformation (strain), *elastically effective strands* are stretched. Extension decreases their conformational degrees of freedom, and this entropic cost results in an increase in free

energy (**Figure 5b**).⁵⁷ Strands that are only attached to the network on one end (dangling ends) or are part of an intramolecular linkage (primary loops) do not bear stress and are thus elastically ineffective despite being connected to the network. In

ideal networks without dynamic bonds or defects, the affine (eq 1) and phantom (eq 2) network models predict the elastic shear stiffness G (stress/strain). In both of these models, increasing stiffness is directly proportional to increasing the number of elastically effective strands:

$$G = k_B T \nu_{\text{eff}} = \frac{\rho_{RT}}{M_S}$$
 (1)

$$G = \left(1 - \frac{2}{f}\right) k_B T \nu_{\text{eff}} = \left(1 - \frac{2}{f}\right) \frac{\rho_{RT}}{M_S}$$
 (2)

where f is the functionality at a junction, k_B is Boltzmann constant, T is absolute temperature, and $v_{\rm eff}$ is the number density of elastically effective network strands. An alternative form of the equations relate G to ρ , the network mass density, and M_s , the number-average molecular weight of a network strand between junctions. The affine model applies a simplifying assumption that crosslink junctions are fixed as if they are pinned in elastic space and therefore move identically to the bulk deformation of the network. However, this is not the case in real networks; network junctions fluctuate and the trajectories of individual junctions vary. The phantom network model captures this statistical variation and makes the assumption that junctions move around mean positions in a Gaussian manner albeit independently of network strain.⁵⁸ The modulus predicted by the phantom network model is always lower than that of the affine network model for equivalent $v_{\rm eff}$, approaching that of the affine model with increasing polymer concentration as junction fluctuation becomes negligible.

Neither the affine nor the phantom network models account for network defects that lower $\nu_{\rm eff}$. To quantify loops and calculate their effect on elasticity, Olsen and Johnson developed Real Elastic Network Theory (RENT). FENT accounts for primary (elastically inactive) and higher-order loops (fractionally elastically active), which exist in a one-to-one ratio and decrease the number of elastically active strands in a network (**Figure 5b**). This theory, coupled with experimental primary loops counting using symmetric isotope labelling disassembly spectrometry (SILDaS), $^{61-63}$ demonstrates good predictive agreement between calculated and measured elasticity for low fractions of loops.

For associative networks, stiffness may be described by the models developed for permanent networks because the bonds exchange without altering the number of crosslinks or junctions. For addition/elimination associative mechanisms, the formation of an intermediate is expected to temporarily *increase* the concentration of effectively elastic strands, but this phenomenon has not been observed experimentally, likely due to the short lifetime of these intermediates. Furthermore, associative mechanisms that proceed by substitution or addition/elimination (rather than metathesis) require that the network is synthesized with an excess of the nucleophilic partner. Therefore, associative networks are often synthesized with a fraction of dangling nucleophilic ends that reduce elasticity.

In a network formed from dissociative dynamic crosslinks, added complexity arises because the number of elastically effective strands depends on the equilibrium constant (K_{eq}) of the dynamic bond. ⁶⁴ To describe the contribution of dynamic bonds to network mechanics, Zhao⁶⁵ and Tibbitt⁶⁶ modified the phantom network model to include K_{eq} . At equilibrium, the conversion of formed crosslinks p can be calculated by eq 3:

$$p = \left(1 + \frac{1}{2cK_{eq}}\right) - \left[\left(1 + \frac{1}{2cK_{eq}}\right)^2 - 1\right]^{0.5}$$
 (3)

where c is the concentration of functional groups. Eq 3 is useful for selecting a relevant dissociative dynamic chemistry through calculation of a "critical equilibrium constant" $K_{\text{eq,c}}$. Flory-Stockmayer theory provides gel point p_c , the conversion at which a polymer solution is crosslinked into a network with a molecular weight of infinity. For a given concentration c, K_{eq} of the crosslink must exceed a threshold $K_{eq,c}$ to produce an infinite network, where p from the modified phantom network model exceeds p_c from the Flory-Stockmayer equation. Similarly, this relationship can be combined with a Van't Hoff analysis $(\ln(K_{eq}) \text{ vs. } 1/T)$ to predict the temperature at which a dissociative network will flow (T_{flow}). Tibbitt showed that values of Keq and shear stiffness obtained by the dynamic phantom network model are consistent with experimental measurements. As with elastic networks, entanglements and network defects will alter network elasticity, limiting the accurate prediction and quantitative analysis of dynamic covalent networks.

2.2 CROSSLINK EXCHANGE KINETICS AND VISCOELASTIC TIMESCALE

Networks based on dynamic bonds are viscoelastic and can flow under conditions that allow the bonds to exchange across macroscopic distances. The temperatures at which this rearrangement occurs, and their timescales, determine the utility of these properties for materials applications and are therefore critical to understand and manipulate. In dynamic covalent networks, the kinetics of bond breaking and formation govern the dynamic bulk properties of the network.

Semenov and Rubinstein established a theoretical foundation for this relationship in reversible networks that can be considered mechanistically dissociative (their "associating polymers" terminology refers to the tendency of the modeled polymers to associate, not to exchange mechanism). They demonstrated that the bond lifetime τ_b , which is the inverse of bond dissociation rate k_d , determines the rate of stress relaxation of a network (characteristic relaxation time τ^* ; the time required for the material to relax stress to 1/e of its initial value). 49,50,67 However, in systems well above the gel point, crosslinks must break and recombine many times before network topology is changed in a way that results in relaxation, effectively slowing network relaxation and increasing apparent activation energy relative to individual bond dissociation rates and activation energies. 67 Experimental studies in dissociative Diels-Alder-based networks have demonstrated that this theory is applicable to CANs. 68,69 Furthermore, Sakai directly observed the bond lifetime of a dissociative boronic acid-diol system using surface plasmon resonance and confirmed that stress relaxation is dominated by crosslinker dissociation but affected by other processes in the network like chain dynamics. 70 For mechanistically associative networks, an analogous relationship between exchange rate $k_{\rm ex}$ and τ is expected, but the situation is further complicated by the fact that stress is proposed to primarily relax through exchanges that form elastically ineffective network defects.⁵³

On the other hand, the rate of bond formation $(k_a \text{ or } k_{\text{ex}})$ determines the rate of gelation⁶⁷ and self-healing⁷¹ after rupture. To our knowledge, the kinetics of self-healing in CANs have not been directly measured and quantitatively compared to k_a or k_{ex} .⁷² In the supramolecular network literature, Scherman has demonstrated this quantitative relationship for a host-guest system using cucurbit[8]uril ternary complexes.¹³

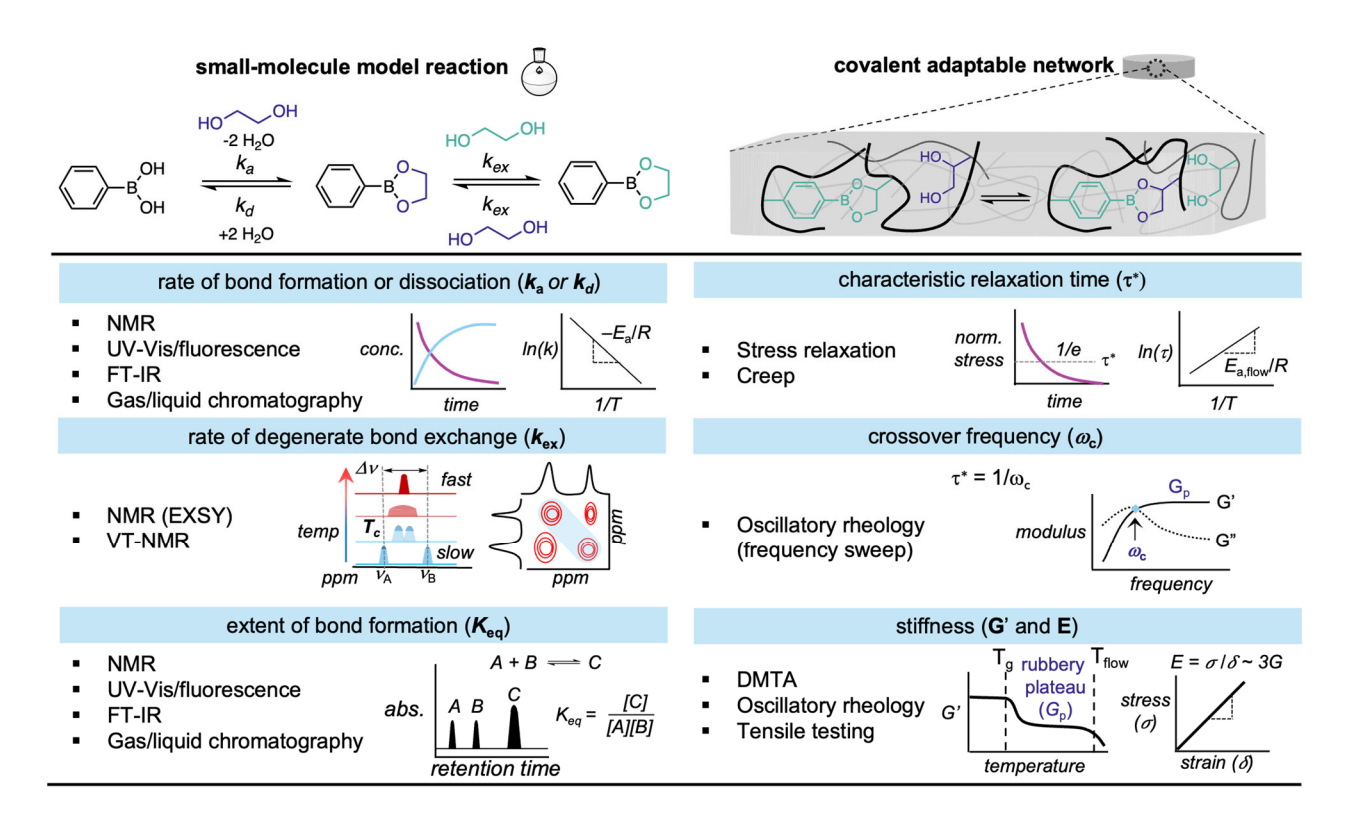


Figure 6. Common techniques for measuring small-molecule reaction kinetic/thermodynamic parameters and network properties.

2.3 MEASUREMENT TECHNIQUES

To understand the relationships between crosslink reactivity and network properties, it is helpful to discuss how molecular and macroscopic parameters are measured. For a comprehensive overview of molecular characterization techniques for polymer networks, the reader is directed to recent reviews. 4,73 Studies often begin with designing small-molecule reactions that resemble the network crosslink exchange, enabling solution measurements. Techniques such as UV-Vis absorption, fluorescence, Fourier-transform infrared spectroscopy (FTIR), gas or liquid chromatography (GC or LC), and nuclear magnetic resonance (NMR) are commonly used to quantify the rate (k) and/or extent (K_{eq}) of bond formation, whereas rapid exchange processes at equilibrium can be measured using techniques such as variable temperature NMR (VT-NMR) or exchange spectroscopy (EXSY) (**Figure 6**). In some cases, the extent of crosslink formation can be measured directly in the network using a solidstate technique like FTIR, ^{68,74} Raman, ⁷⁵ or ssNMR^{76,77} spectroscopy.

The mechanical properties of CANs that will be discussed in this Perspective are measured using dynamic mechanical analysis as well as rheology at constant strain (stress relaxation) or stress (creep). These experiments provide information about the stiffness of the network and the timescale of network rearrangement. Oscillatory shear rheology yields shear storage (G') and loss (G'') moduli, describing the material's ability to store and dissipate energy, respectively. In a frequency sweep, the crossover between G' and $G''(\omega)$ represents the timescale at which a material transitions from solid-like (oscillations faster than the material's characteristic timescale for rearrangement) to liquid-like (oscillations slower than that timescale). These measurements provide a significant amount of data, but the timescale of

many CANs is too slow to reveal crossover within an experimentally accessible frequency range.

As a result, stress relaxation measurements, which measure the dissipation of energy over time following a step strain, are commonly used in this field. Stress relaxation experiments in dry networks typically require elevated temperatures to both overcome the glass transition temperature ($T_{\rm g}$), enabling segmental motion, and to achieve crosslink exchange on a reasonable time scale (seconds to hours). In gels, the presence of solvent (low-volatility solvents such as DMSO or propylene carbonate), plasticization lowers the $T_{\rm g}$ and stress relaxation can be measured at lower temperatures.

Normalized stress relaxation data may be fitted to one of several models to determine a characteristic relaxation time (**Figure 7a**). A simple single-element Maxwell model, which models viscoelastic materials as an elastic spring and viscous dashpot in series, is often a reasonable starting point (**Figure 7b**). For systems that do not exhibit Maxwellian behavior, a Kohlrausch-Williams-Watt (KWW) stretched exponential, which applies a constant β between 0 and 1, may better represent the data (**Figure 7c**). Here, lower β values indicate broader distributions of relaxation modes. Alternatively, a multi-element Maxwell model may be well suited to systems with more than one type of exchange process (**Figure 7d**). If τ^* values are measured at multiple temperatures, the network flow activation energy (E_a) is determined through the Arrhenius relationship:

$$\tau^*(T) = Ae^{-\frac{E_a}{RT}} \tag{4}$$

where R is the ideal gas constant, T is the temperature, and A is the pre-exponential factor. The flow activation energy provides insight into the temperature sensitivity of the network rearrangement, and changes in slope may either imply a change

in mechanism for the exchange reaction⁷⁶ or a change in the rearrangement-limiting process (crosslink exchange vs. segmental dynamics). Evans has observed the latter scenario using measurements over a broad temperature range (200 °C).⁷⁷

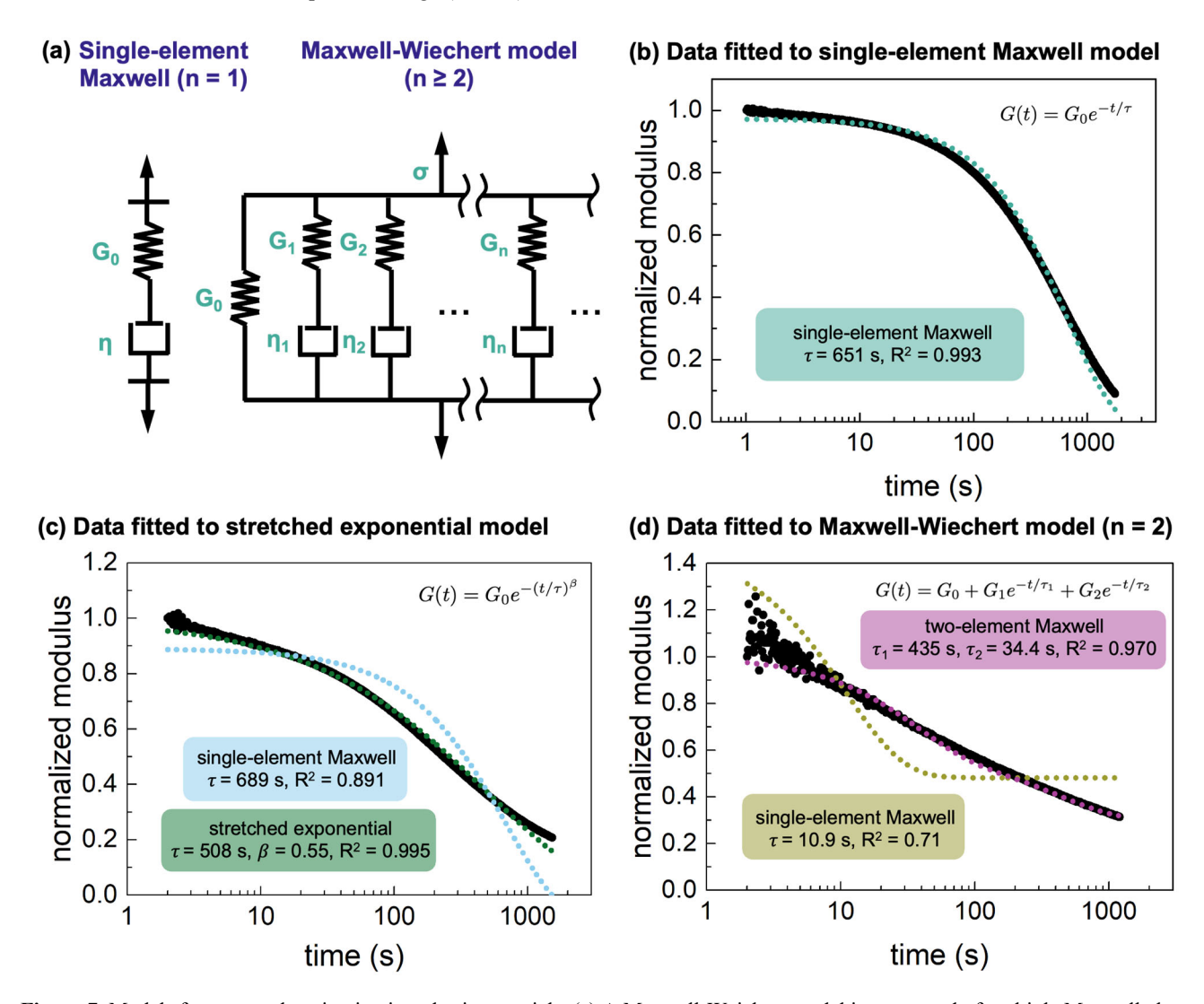


Figure 7. Models for stress relaxation in viscoelastic materials. (a) A Maxwell-Weichert model is composed of multiple Maxwell elements in parallel and captures multiple modes of stress relaxation. (b) Example of data fitted to a single-element Maxwell model. (c) Example of data better represented by a stretched exponential. (d) Example of data better represented by a two-element Maxwell model.

As an alternative to stress relaxation, creep measurements, which measure the deformation of a material over time in response to constant stress, have been recommended for dry networks with slow timescales because these measurements are not limited by the torque resolution of the instrument.⁸¹ The resulting creep rate ($\dot{\varepsilon}$) may also be analyzed by the Arrhenius equation.^{55,79}

Many studies compare the small-molecule E_a derived from Arrhenius analysis to the CAN flow E_a . While the network E_a is expected to be higher than the small-molecule value based on theory, 67,81 the magnitude of this difference depends on the polymer matrix in ways that are not fully understood. $^{82-85}$ Possible explanations include matrix hydrophobicity or polarity in the case of mechanisms that involve charged intermediates, and entropic barriers to rearrangement imposed by rigid backbones.

Several studies of physical networks have demonstrated time-crosslinker superposition (TCLS), in which the frequencydependent mechanical responses of different networks overlap when they are scaled by molecular parameters such as dissociation rate or activation energy (Figure 8a). 10,13 This superposition confirms that networks with different crosslinkers rearrange through analogous mechanisms and that crosslink dissociation controls rearrangement. It should be noted that the polymer networks used in those studies are crosslinked with metalligand or host-guest interactions. Time-crosslinker superposition has yet to be demonstrated for CANs with different crosslinks, which may be ascribed in part to their more complex multistep exchange mechanisms. We attempted TCLS on frequency sweeps obtained from four distinct boronic ester gels and found that the curves did not superimpose when scaled by the boronic ester hydrolysis rate constants or activation energies (Figure 8b).86 The rate-limiting step of boronic ester hydrolysis can change depending on many factors including pH, solvent, and structure of the substrates.^{37,87} The lack of superposition indicates a discrepancy in the translation from small-molecule parameters to macroscopic network properties. While TCLS may be possible in other CANs with single-step mechanisms, in this

Perspective we draw inspiration from physical organic chemistry to suggest other methods for analyzing structure-property-reactivity relationships in CANs.

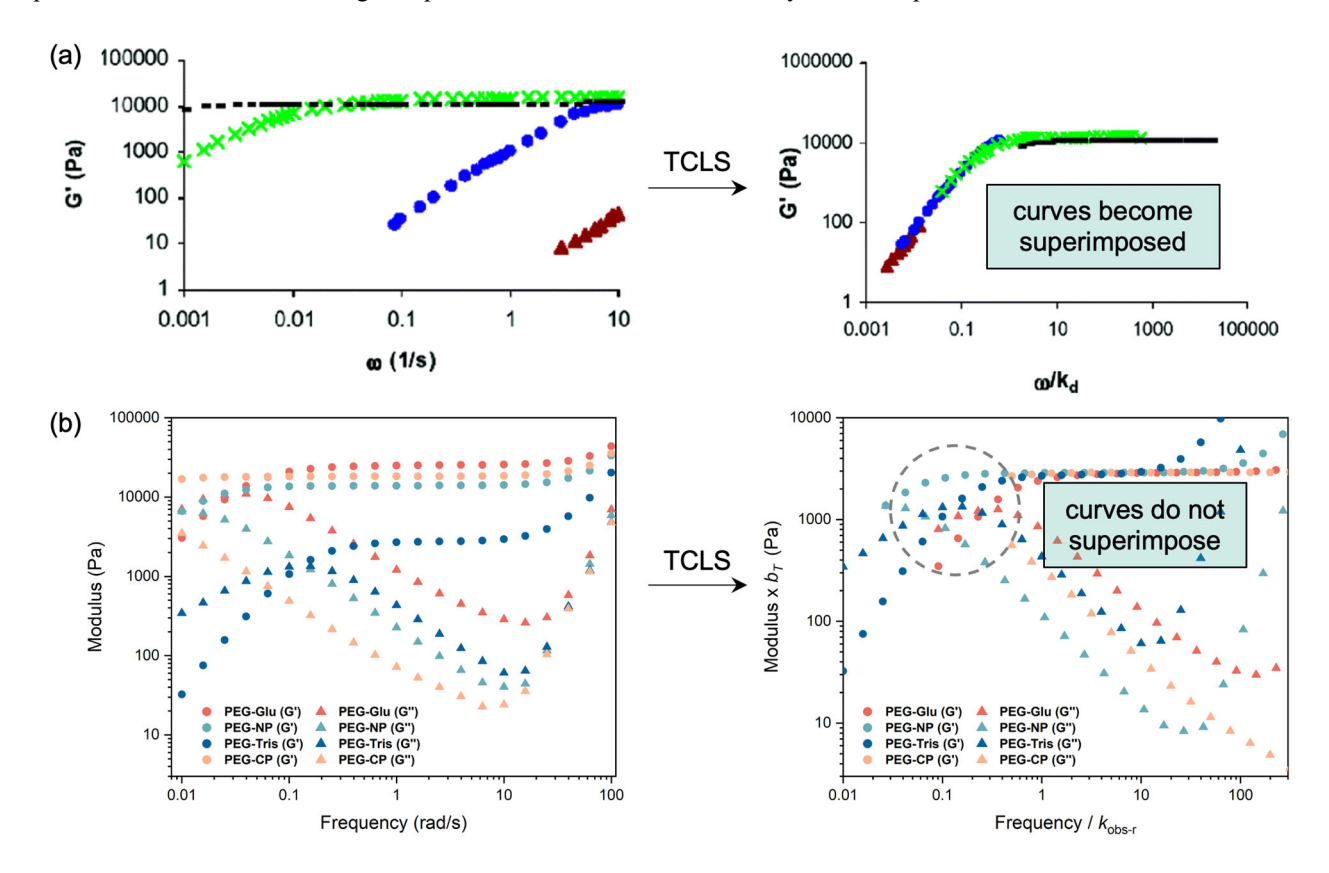


Figure 8. Time-crosslinker superposition of frequency curves for analogous but structurally-different crosslinkers. (a) Successful application of TCLS in a supramolecular metal-ligand network based on the small-molecule k_d values. Reprinted with permission from ref. ¹⁰. Copyright 2005 American Chemical Society. (b) Frequency sweeps from four different boronic acid-diol crosslinked networks do not superimpose based on k_d . Adapted with permission from ref. ⁸⁶. Copyright 2022 American Chemical Society.

3. STRATEGIES TO MODULATE MOLECULAR REACTIVITY AND NETWORK PROPERTIES

As CANs are based upon chemical reactions, it stands to reason that the same tools that are used to understand and optimize reactions can be applied to these materials. In the realm of reaction optimization and catalyst design, researchers have harnessed quantitative descriptions of molecules to understand and improve reactivity and selectivity.88-90 The earliest form of these methods, linear free energy relationships (LFERs), use experimentally- or computationally-derived data to reveal a trend between specific molecular features in a series of substrates or catalysts and reaction rates or selectivities. 91 By comparing the magnitude or direction of the trend to the literature, one may extract mechanistic insight about the reaction; furthermore, one may use this trend to predict the performance of a new substrate or catalyst. Recent years have seen the development of more sophisticated ways to analyze, describe, and predict chemical space.89,90

In comparison, the application of such quantitative structure-reactivity relationships to CANs is still in its infancy. A key challenge in directly relating small-molecule parameters (k_a , k_d , K_{eq} , k_{ex} , E_a) to macromolecular properties (G, τ^* , flow E_a , ω) is the fact that small-molecule reactions cannot replicate the pol-

ymer matrix environment and the perturbations induced by mechanical forces.³³ Here we review several examples comparing small-molecule reactivity and network properties to demonstrate the potential and limitations of such analyses. We highlight chemical design principles that can be used to systematically manipulate and understand reactivity and show how these principles can be translated to the design of polymer networks. As this field continues to develop, we anticipate that the parametrization of dynamic covalent bonds will prove an enabling tool for developing quantitative structure–reactivity–property relationships.

3.1 POINT SUBSTITUTIONS

One of the most straightforward methods to modify reactivity and develop structure-property relationships is to minimally alter the electronic or steric environment surrounding a reaction center, which we here refer to as point substitutions. When comparing two CANs with the same exchange chemistry but different partners, researchers often qualitatively rationalize the direction and extent of change that these substitutions confer based on the mechanism of the reaction. However, several recent examples go beyond pairwise comparisons to study a series of CANs with point substitutions that are well-suited to traditional LFER parameters (Table 1). These studies provide the

opportunity to use the resulting structure-reactivity-property relationships quantitatively and predictively.

Electronic effects. Hammett parameters capture the effect of installing electron-donating and electron-withdrawing groups on reactivity. ⁹² Several recent examples demonstrate the application of Hammett relationships to a series of dynamic covalent bonds and then seek to translate this trend to the corresponding CANs. These examples reveal considerations that arise when point substitutions are introduced in a network context.

Smulders demonstrated a Hammett-based approach to tuning the viscoelastic parameters of an imine CAN.³¹ The dianilines **Table 1. Common parameters for LFERs.**

shown in **Figure 9a** are commercially available and differ in nucleophilicity based on the electronics of the bridging group. Electron-withdrawing substituents decrease the nucleophilicity of the p-anilines and -donating substituents increase it; these properties manifest as an increase in both reaction rate (k_a) and equilibrium constant (K_{eq}) for transimination with more electron-rich anilines. When plotted as a function of σ_{para} , $\log(k)$ and $\log(K_{eq})$ exhibit a linear trend spanning two orders of magnitude, with individual deviations that the authors attribute to solubility differences (**Figure 9b**).

Substituent parameter	Effects	Reference reaction
σ para	Electronics	0 0
σ_{meta}	Electronics	$\chi \stackrel{\text{(i)}}{=} OH + H_2O \stackrel{K_X}{=} \chi \stackrel{\text{(i)}}{=} O^{\Theta} + H_3O$
σ+	Resonance stabilization (negative charge)	$X \longrightarrow {}^{OH} \xrightarrow{\kappa_X} {}^{H^{\oplus}} {}^{+} X \longrightarrow {}^{O^{\ominus}}$
σ-	Resonance stabilization (positive charge)	$X \longrightarrow X \longrightarrow$
Es	Sterics	О _{ks} О Д → Д + МеОН
σ^{\star}	Polarity	R ² OMe R ² OH E _s measured for acid hydrolysis σ* measured for difference between acid and base hydrolysis

(a) transimination excess imine metathesis (c) (b) 100 E_a SDA 80 FDA E_a [kJ/mol] 60 KDA 40 --3 SDA 0.0 0.2 0.4 0.6 0.7 0.0 0.1 0.5 0.6 σ

Figure 9. (a) The small-molecule transimination with tunable dianilines used to measure k_1 and K_{eq} and the imine metathesis mechanism proposed to occur in the material. By the principle of microscopic reversibility, the cyclic intermediate undergoes a retro-[2+2] to afford the degenerate exchange products. (b) Hammett plot of K_{eq} and k_1 as a function of σ_{para} . (c) Hammett plot of flow E_a and strain after constant stress as a function of σ_{para} . Reprinted with permission from ref. ³¹. Copyright 2021 The Royal Society of Chemistry.

Based on the small-molecule studies, one would expect that networks based on electron-rich anilines would have lower flow activation energies and deform more upon applied stress (creep). In contrast, more electron-rich dianiline crosslinkers provide networks with *slower* stress relaxation, *higher* flow E_a , and less creep (Figure 9c). It is likely that the mechanism of exchange differs between the small molecule system and the bulk network: the stoichiometry of aniline to imine in the smallmolecule system promotes a transimination mechanism, whereas the network is synthesized without free amine, biasing the system towards imine metathesis. Therefore, the electronic trends reflect electrophilicity of the imine rather than nucleophilicity of the aniline. Nevertheless, the network properties related to viscoelasticity exhibit a linear trend with respect to σ_{para} in the first demonstration that vitrimers can be directly analyzed by LFERs.

Winne and Du Prez investigated how electronics affected the thermodynamics and kinetics of base-catalyzed reversible thia-Michael addition in CANs derived from arylpropynones. 93 Rate constants and activation energies for their small-molecule model system were obtained by ¹H NMR. The resulting rate constants were significantly affected by the electron-donating or -withdrawing nature of the para substituent on the aromatic ring, with -NO₂ providing the fastest exchange and -NMe₂ the slowest by almost three orders of magnitude. The positive, linear correlation obtained in the Hammett analysis supports a common mechanism of exchange and implicates an increase in negative charge in the transition state (Figure 10a). While the authors attribute this effect to stabilization of the conjugate addition transition state by electron-withdrawing groups, the trend is also consistent with stabilization of the deprotonation step in conjugate elimination.

While these molecular trends were generally reproduced in the CANs, with electron-withdrawing substituents providing faster relaxation than electron-donating ones, unlike the vitrimers studied by Smulders, this system is not amenable to a simple Hammett analysis. We plotted characteristic relaxation time at 130 °C and flow E_a as a function of Hammett parameter σ_{para} and observed the expected trends, but limited adherence to a linear fit (R^2 values ~0.6, **Figure 10b-c**).

Several reasons may underlie these deviations. Since the thia-Michael CANs rearrange by a dissociative mechanism, K_{eq} and thus crosslink density depend on the temperature and structure of the crosslink; these differences are reflected in the variable stiffnesses of the materials. With sufficient information about crosslink conversion and gel point, Bowman and Wang have shown that it is possible to apply Semenov–Rubenstein theory to dissociative CANs, which could in principle be used to convert the measured characteristic relaxation times to bond lifetimes. ^{68,69} In addition to differences in topology, this reaction requires a base catalyst, and the mobility of the catalyst in the matrix may affect the rate of network rearrangement.

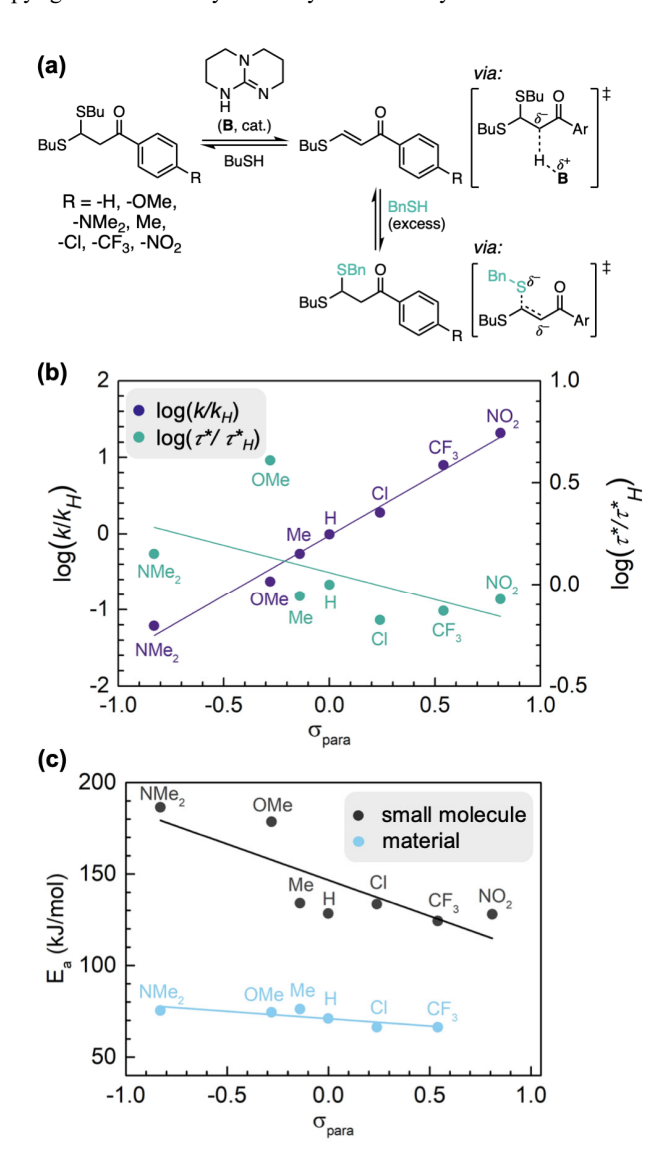


Figure 10. (a) Thioacetal exchange mechanism. (b) Hammett plot for small-molecule exchange rates and stress relaxation times as a function of σ_{para} . (c) Hammett plot for small-molecule and network flow activation energies as a function of σ_{para} . Data extracted from ref. 93 using WebPlotDigitizer. 94

In a c atalyst-free thia-Michael CAN based on benzalcyanoacetate acceptors, Rowan focused on the effect of electronic substitutions on the thermodynamics of the dynamic bond. To A positive slope in the Hammett plot of $\log(K_{\rm eq}/K_{\rm H})$ vs. $\sigma_{\rm para}$ for the β -aryl substituent suggests that electron-withdrawing groups favor Michael adduct formation (**Figure 11**). A Van't Hoff analysis reveals that the differences in equilibrium have enthalpic origins. This trend was then translated to CANs, where the extent of bond formation could be estimated in the solid state by Raman spectroscopy. Again, the trend in extent of bond formation with respect to $\sigma_{\rm para}$ was more complex in the material. Acceptors with low $K_{\rm eq}$ were unable to form networks with sufficient integrity for mechanical tests, as expected, 66 while the rubbery plateau moduli and thermal transition to flow could be qualitatively attributed to the thermodynamics of the dynamic bond. However, the dynamic reaction induces phase separation in these networks, which complicates straightforward comparison to molecular parameters and illustrates the complexities introduced by macromolecules. The same general trend in K_{eq} was observed by Rosales in a complementary study of the same dynamic bond under aqueous conditions, where the effect of electron-withdrawing groups was attributed to an increase in the conjugate addition rate (k_a) with little effect on the conjugate elimination rate (k_d) . As a result, hydrogels based on an electron-poor acceptor were stiffer, but the rates of stress relaxation (governed by k_d) were approximately the same.

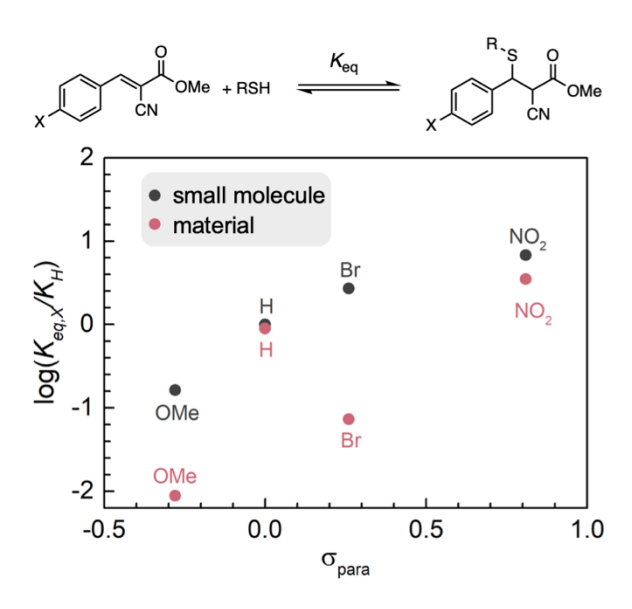


Figure 11. Hammett plot for small-molecule and (estimated) network E_a in a thia-Michael network as a function of σ_{para} .

Steric effects. The reactivity of dynamic bonds can also be probed and manipulated by modifying their steric environment. Steric effects can provide a straightforward way to distinguish between associative and dissociative mechanisms. The addition of steric hindrance will tend to decelerate associative exchange because the transition state is more congested than the reactants (Figure 12a). This effect is used to develop Taft parameters, which are based on the rate of acid-catalyzed ester hydrolysis. In contrast, bulky substituents will accelerate a dissociative mechanism by raising the energy of the starting materials relative to the transition state. The evaluation of multiple substrates through a LFER can be used to assess which mechanism is operative, or whether a change in mechanism occurs corresponding to a change in slope.

(a)
$$H_{0}^{\oplus}$$
 \longrightarrow H_{0}^{\oplus} H_{0}^{\oplus} \longrightarrow H_{0}^{\oplus} $\xrightarrow{H_{0}^{\oplus}}$ $\xrightarrow{H_{0}^{\oplus}}$ $\xrightarrow{H_{0}^{\oplus}}$ $\xrightarrow{H_{0}^{\oplus}}$ $\xrightarrow{H_{0}^{\oplus}}$ $\xrightarrow{H_{0}^{\oplus}}$

increasing steric bulk increases ΔG^{\ddagger}

(b)
$$\begin{bmatrix} \begin{pmatrix} v \\ h \end{pmatrix} & \begin{pmatrix} v \\ h \end{pmatrix} \end{bmatrix} \begin{bmatrix} v \\ h \end{pmatrix} \begin{bmatrix} v \\ h \end{pmatrix} \begin{bmatrix} v \\ h \end{bmatrix} \begin{bmatrix} v$$

increasing steric bulk decreases ΔG^{\ddagger}

Figure 12. Increasing steric hindrance of a crosslink will tend to (a) decrease the rate of associative exchange, and (b) increase the rate of dissociative exchange.

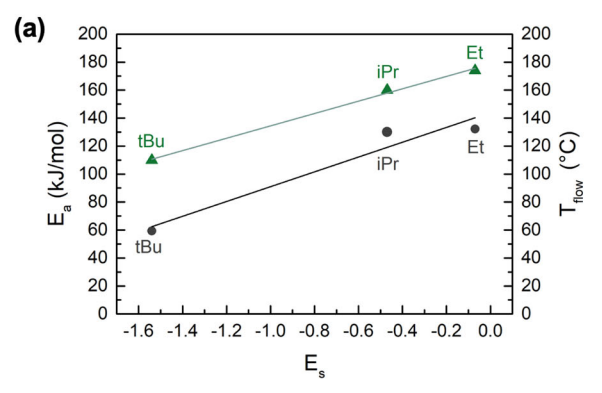
In transesterification-based vitrimers, Terentjev observed 38 kJ/mol higher flow E_a when comparing an ester with a β -methyl group to one without this substituent, as expected for an associative mechanism. ⁹⁶ Unexpectedly, the more sterically hindered vitrimers underwent creep at a *lower* temperature, which was ascribed to its lower rubbery modulus and thus less crosslinked structure. This example highlights the importance of network topology and multiple forms of measurements when comparing a series of CANs.

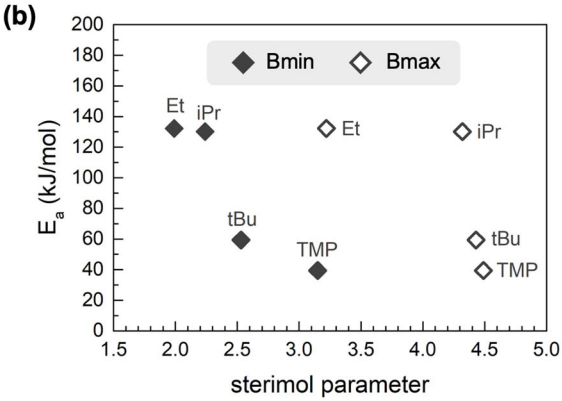
The dissociation of *N*-alkylureas is illustrative of a dissociative mechanism that has been tuned by steric effects in CANs. ^{97,98,74,99} Cheng showed that hindered urea bonds (HUBs) exist in an equilibrium with their dissociation products, isocyanate and amine (**Figure 12b**). The bulky substituent raises the energy of the urea by enforcing a geometry that disrupts the conjugation between the N lone pair and the carbonyl p orbital, lowering the activation barrier to dissociation. ¹⁰⁰ Both Cheng and Rowan have taken advantage of this effect to design self-healing polyurea networks with tunable mechanical properties. ^{97,98,74}

Here, we focus on Rowan's study, which examined the effect of N-alkyl substituent on terminal flow temperature and stress relaxation in polyurea thermosets without significant changes in $T_{\rm g}$ or rubbery plateau modulus. The equilibria between urea and isocyanate in the bulk networks were monitored by temperature-dependent FTIR, which revealed that bulky substituents increase the extent of dissociation and decrease in the temperature at which dissociation occurs. Furthermore, the authors derived flow $E_{\rm a}$ from stress relaxation data for a series of CANs. We plotted flow $E_{\rm a}$ and $T_{\rm flow}$ against the Taft parameter and observe a modest trend that would benefit from additional data points to strengthen the analysis (**Figure 13a**). However, Taft parameters rely on experimental data. The tetramethylpiperidine substituent has not been parametrized and therefore cannot be evaluated in relation to the other substrates.

Computational parametrization tools such as DBSTEP, an open-source software developed by Paton, allow the steric properties of any substituent to be determined *in silico*. ¹⁰¹ Compared to Taft parameters, Sterimol parameters typically better describe asymmetric substituents because they capture distances along principal axes. ¹⁰² We entered Cartesian coordinates for four small-molecule ureas into DBSTEP to obtain Bmin, Bmax, L, and % buried volume parameters for all four substituents and plotted Rowan's reported E_a values against them (see Supporting Information for details). The results in

Figure 13b-c again capture the overall trend but could not predict the similar E_a of Et and iPr. Alternatively, a change in slope in an LFER can indicate a change in mechanism; the absence of terminal flow and increase in modulus at higher temperatures for the Et-based network could suggest some amount of associative exchange, in addition to the proposed degradation. ¹⁰³ Based on these data, we hypothesize that a substituent with intermediate Bmin or Bmax parameters would lead to a material with intermediate E_a . We extracted Sterimol parameters for a range of alkylamines with similar electronics and identify pyrrolidine and tetramethylpyrrolidine as potential substituents that would provide intermediate flow E_a and T_{flow} .





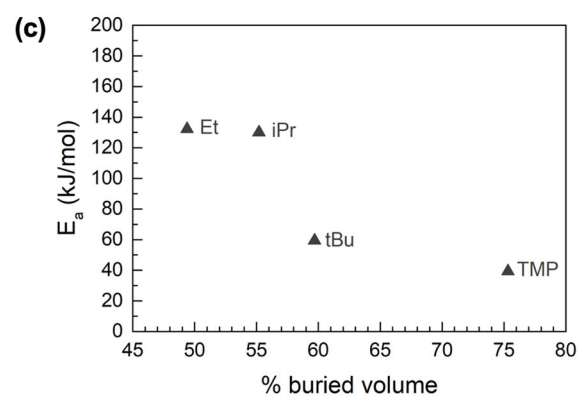


Figure 13. (a) Taft plots showing the relationship between N-alkyl substituent size, flow E_a (green triangles), and T_{flow} (black circles). (b,c) Analysis of flow E_a using computationally derived (b) Sterimol parameters and (c) % buried volume.

In this section, we have presented several examples of tuning network properties using point substitution and discussed how the application of this design principle lends itself to establishing LFERs for polymer networks. We encourage researchers in

the field to consider whether LFERs are applicable to systems under study and to test the predictive power of these relationships. Systems that deviate from linearity may suggest the contribution of matrix effects on network rearrangement, such as chain flexibility, phase separation, crystallinity, or entropic effects. 104 In Section 4, we discuss considerations in the design of small-molecule model systems and polymer networks to improve the strength of these relationships. We also encourage researchers to use the computational tools developed for reaction optimization and asymmetric catalysis to explore functional groups that may not be described by traditional Hammett or Taft parameters. 88-90 Point substitutions offer a structurally conservative and often synthetically accessible method to alter crosslink structure and tune macromolecular properties over a broad range; the development of LFERs for CANs will improve predictability in the form of quantitative structure-reactivityproperty relationships.

3.2 INTERNAL CATALYSIS

Internal catalysis relies on proximity-induced enhancement of reactions of nearby functional groups. These groups facilitate reactivity by stabilizing transition states and creating lower-energy reaction pathways (enthalpically favored) or by increasing the chance of reaction through proper orientation of reactants (entropically favored). 105,106 As a result, inductive, ionic, electrostatic, dipolar, or covalent interactions can accelerate exchange, with the proximity of the respective catalytic group being critical. 107,108 Groups that are considered mild acids or bases can have pronounced effects on reactivity that typically requires strong acid or base external catalysts. In these studies, control systems lacking the internal catalyst or positioning it less favorably are typically designed to provide mechanistic support. The nature of internal catalysis is also important for its effect on network topology. Internal acid or base catalysis that involves Hbonding to enhance electrophilicity or nucleophilicity, respectively, will not affect the mechanism of reconfiguration (Figure 14a). In contrast, neighboring group participation that involves intramolecular cyclization will convert a mechanistically associative process such as transesterification to a topologically dissociative network rearrangement (Figure 14b). Here, we focus on the first form of internal catalysis.

Figure 14. Two forms of internal catalysis for transesterification of a benzoic ester. (a) H-bonding by an adjacent phenol lowers the activation energy without altering the exchange mechanism. (b) Neighboring group participation that generates a phthalic anhydride intermediate results in a topologically dissociative exchange mechanism. 109

Internal catalysis can mediate dramatic rate accelerations with minimal structural modifications to the dynamic bond. Wulff showed that neighboring amines on boronic esters significantly accelerate the transesterification of boronic esters by

lowering the barrier to proton transfer.¹¹⁰ Guan translated this effect to self-healing boronic ester networks.¹¹¹ In a small-molecule model system, the authors observed a difference of about 5 orders of magnitude for exchange rates in the presence and absence of the internal catalyst (**Figure 15a**). This effect was translated to polymer networks using divalent boronic ester crosslinkers with and without proximal amines and provided greater malleability and self-healing ability in the material with internal catalysis. Guan further expanded this design to silyl ether-based CANs with internal amine catalysts.¹¹²

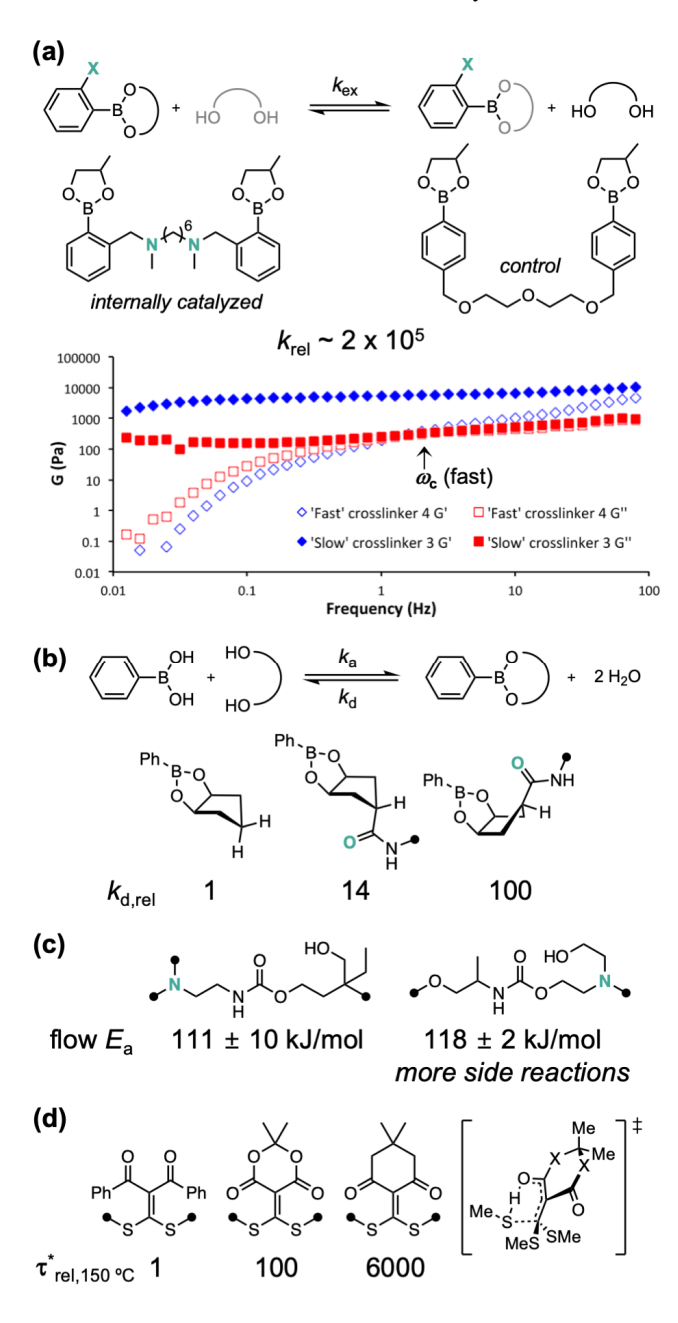


Figure 15. Examples of internal catalysis translated to CANs. (a) Internal base catalysis by Wulff-type boronic esters and corresponding frequency sweep of boronic ester CANs. Reprinted with permission from ref. ¹¹¹. Copyright 2015 American Chemical Society. (b) Internal catalysis of boronic acid—diol reversible condensation by amides. (c) Internal catalysis of urethane exchange by amines. (d) Internal catalysis of thiol conjugate addition—elimination by carbonyls.

While internal base catalysis by proximal amines in arylboronic acids and esters is well established, 110,113,114 our studies of boronate ester gels revealed that the amide group used to conjugate diols to polymers can also act as an internal catalyst (**Figure 15b**). 86 By comparing the small-molecule reactivity of diols with and without amides, we showed that the internal catalytic effect is more pronounced for hydrolysis than for esterification, resulting in lower $K_{\rm eq}$ values in the presence of amides. These trends were borne out in the stress relaxation and stiffness of the corresponding gels. Because effective internal catalysis relies on a decrease in entropy, these effects are highly sensitive to the placement of the internal catalytic group relative to the reactive site, as exemplified by a cyclopentanediol substrate with the amide syn or anti relative to it.

The effect of the location of the internal catalyst has been demonstrated for other dynamic bonds. Cramer, Hillmyer, and Dichtel previously reported catalyst-free polyhydroxyurethane vitrimers based on TREN as the multifunctional monomer. Guerre, Sardon, and Du Prez proposed that exchange in these networks is internally catalyzed by the tertiary amine in TREN. He while networks with amines on either the nitrogen or oxygen side of the carbamate displayed similar flow E_a values in stress relaxation measurements (111–118 kJ/mol), the latter design underwent urea formation during reprocessing, suggesting that the placement of the internal catalyst can affect the prevalence of side reactions (**Figure 15c**).

In PDMS vitrimers based on the conjugate addition-elimination of thiols to electron-deficient dithioalkylidenes,¹¹⁷ we found that acceptors derived from cyclic 1,3-diketones and diesters provided significantly faster stress relaxation compared to those derived from their linear counterparts (**Figure 15d**).¹¹⁸ Based on DFT, this effect was rationalized by the ability of the carbonyl to facilitate proton transfer to and from the thiol in a closed transition state. Cyclic acceptors enforce a conformation that stabilizes this transition state. However, we have since observed that this conjugate addition-elimination operates by a different mechanism in aqueous environments, highlighting the importance of solvent/matrix in these comparisons.

3.3 PHOTOSWITCHABLE DYNAMIC COVALENT CROSSLINKS

The case studies discussed above reveal the sensitive relationship between crosslink structure and network properties, offering design principles to tune network through molecularlevel engineering. An appealing feature of dynamic covalent bonds is their stimuli-responsiveness, which offers the potential to control network mechanics in situ. Common stimuli include pH, small-molecule analytes, temperature, and light. Light is a particularly attractive stimulus because it can be applied externally with spatial and temporal control. By coupling the reactivity of crosslinks to a light-responsive molecule, network mechanics can be precisely manipulated after fabrication. While certain cycloadditions and bond homolyses can be directly induced by light, red-shifting the wavelengths required for photocontrol inherently lowers the energy available for dynamic bonding. 119 Here, we focus on reversible photocontrol based on the effect of photoswitches on dynamic covalent bonds (Table 2). These designs enable decoupling of the photoreaction and the thermally-controlled dynamic covalent crosslink.

Table 2. Photocontrollable dynamic covalent bonds and conditions used in networks.

Dynamic bond	Mechanism	Solvent conditions	Refer- ences
Diels-Alder cy- cloaddition	Dissociative	Neat	120,121
Other cycloadditions	Dissociative	Aqueous Neat	122–124
Imine condensa- tion	Dissociative	Neat	125
Boronic ester condensation	Dissociative	Aqueous	126,127
Boronic ester transesterifica- tion	Associative	Neat	128
Transthioesterifi- cation	Associative	Neat	129
Allyl sulfide ex- change	Associative	Aqueous Neat	130–132
Disulfide ex- change	Associative or dissociative	Aqueous Neat	133

Branda first demonstrated that reversible Diels–Alder cycloadditions could be controlled by the isomerization of a dithienylethene photoswitch and highlighted the wavelength tunability of this approach. 134 In the open isomer, the photoswitch can engage in the cycloaddition; when the adduct is switched to the closed state, it is unable to undergo retro-Diels–Alder. Hecht then modified this design 135 and applied it to conditionally selfhealing polymethacrylate CANs (**Figure 16a**). 121 Healing of a scratched film was mediated by both heating and 365-nm irradiation. With the photoswitch its open (reactive) form, $T_{\rm flow}$ above 100 °C is observed; the closed (locked) form displays a

smaller drop in modulus at a similar temperature but does not flow. However, the materials display very similar mechanical properties below $T_{\rm flow}$.

Extending this concept to a lower-temperature dynamic bond, Hecht synthesized photoswitchable aldehydes to achieve different condensation rates with either hydrazides or amines, which was then translated to photocontrol the self-healing rate of PDMS CANs (**Figure 16b**). ¹⁶ While several classes of photoswitches were explored, a diarylethene provided the greatest difference in imine formation rate (about 1 order of magnitude) and was bistable. Interestingly, while the goal of this design was to photoswitch crosslink formation kinetics and thus self-healing rates, *G*' of the faster-reacting form is ca. 5-fold higher, suggesting that the aldehyde-imine equilibrium constants are also affected by the photoswitch.

Inspired by this work and the well-documented tunability and aqueous compatibility of the boronic ester dynamic bond, 38,136 our lab sought to photocontrol the mechanics of boronic ester hydrogels. Azobenzenes were selected based on their aqueous compatibility, tunability, and modularity. 137 We discovered that ortho-azobenzeneboronic acids bind diols more strongly in the Z conformation than in the E conformation (Figure 16c). 138 Detailed experimental and computational studies revealed the origin of this isomerization-driven change in binding constant and enabled predictive design based on the sterics and H-bonding ability of ortho groups. 127 When a fluorinated ortho-azobenzeneboronic acid was appended to 4-arm PEG with a complementary polyol, K_{eq} for boronic ester formation in the E isomer fell short of the gel point, while isomerization to the Z isomer with green light provided a hydrogel with G' of ~ 2 kPa. Interestingly, while the stiffness of these hydrogels was reversibly photocontrolled with solely visible light, stress relaxation was constant. This decoupling of stiffness and stress relaxation had not been previously demonstrated in a single material.

Figure 16. Examples of photoswitchable dynamic covalent bonds applied to CANs. (a) Diarylethene conformation turns on and off a reversible Diels—Alder reaction. (b) Diarylethene conformation controls the rate of imine formation. (c) Azobenzene conformation controls the binding of diols to boronic acids, enabling hydrogels with reversibly photocontrolled stiffness. (d) Acylhydrazone conformation controls the activity of an internal catalyst for boronic ester transesterification.

To complement this work, we were inspired to develop photoswitches that can be used to control stress relaxation independent of storage modulus. Rather than manipulating both k_a and kd in a dissociative dynamic crosslink, in analogy to Rosales' work, 95 we envisioned that an associative mechanism would enable photoswitchable control over $k_{\rm ex}$ without affecting network topology and thus stiffness. Based on Wulff's studies of internal catalysis in boronic ester transesterification, we designed a bidirectional hydrazone photoswitch that reversibly gates an internal base catalyst (**Figure 16d**). ¹²⁸ The resulting k_{ex} is altered by over 4 orders of magnitude based on the photoswitch conformation. In a poly(caprolactone) network, this rate difference translated to a shift in the crossover frequency ω_c without any change in the plateau modulus. While an exciting proof of concept, many practical challenges (synthetic accessibility, hydrolytic stability) must be addressed before this system can be applied to a functional material.

4. CONCLUSIONS AND OUTLOOK

In this Perspective, we have focused on several studies that systematically evaluate a series of dynamic covalent crosslinks and correlate the trends in reactivity to the mechanical properties of the corresponding CANs. We propose that analyzing these structure-reactivity-property relationships using LFERs will improve our ability to design CANs with targeted mechanics, and in addition, may reveal mechanistic insight that is challenging to obtain through more direct measurements. We also highlight the significant impact that internal catalysis and photoswitches can have on reactivity and the translation of these effects to CANs.

We anticipate that the systematic study of CANs through quantitative structure-reactivity-property relationships will enable the design of rapid but high- E_a dynamic bonds ideal for reprocessable, creep-resistant elastomers and thermosets. By understanding exchange mechanisms in detail, it will be possible to design photoswitches that dramatically alter the physical properties of hydrogels for biomedical studies. Beyond photocontrol, a particular interest of our lab, the design principles extracted from these relationships will accelerate the development of materials with targeted properties and responses to other stimuli. We also envision that the marriage of mechanochemistry¹³⁹ and CANs will enable an exciting new class of materials whose dynamic properties change as a function of force. ¹⁴⁰

As physical organic and synthetic chemists working in the field of CANs, we offer below several recommendations for future studies that seek to develop these structure-reactivity-property relationships. Furthermore, we suggest advances in measurement science that would greatly impact this field by enabling direct measurement of crosslink reactivity in CANs.

4.1 THE DESIGN OF SMALL-MOLECULE MODEL SYSTEMS

In order for small-molecule model systems to be useful for predicting network trends, we recommend that the following criteria are considered:

 Because dynamic covalent bonds are so sensitive to structure, the small molecule systems must be structurally relevant to the material and not overly simplified.⁸⁶

- 2. The conditions used for the small-molecule model system should be as relevant as possible to the polymer system. Factors such as the polarity of the solvent, presence or absence of water, and even stoichiometry³¹ and spectator ions^{3041,86} can affect the mechanism and rate of exchange. When differences are required by experimental constraints (e.g. reasonable viscosity, solubility, or reaction rates), they should be noted and rationalized.
- 3. When synthetically/commercially accessible, structural modifications that lend themselves to LFERs are recommended. When simple electronic and steric point substitutions with corresponding literature parameters are not possible, computationally or spectroscopically derived parameters^{88,89} should be considered.

4.2 MACROMOLECULAR CONSIDERATIONS

In applied settings, the network components and their assembly will be dictated by practical considerations such as feed-stock availability and cost, the target properties of the network, cure rate and conditions, etc. For fundamental studies like many of the ones discussed here, however, these constraints are less relevant and designs that offer the best possible comparison between networks and between experiment and theory may be prioritized:

- 1. The vitrimer matrix (T_g , polarity, molecular weight) can profoundly affect viscoelasticity. ^{84,141} Deviations from Arrhenius behavior are observed near T_g , ⁸¹ phenomena like phase separation and crystallinity that are not observed in small-molecule solution studies also impact the ability of the dynamic bonds to engender network rearrangement. ^{142,143,75,32} Therefore, if one wishes to focus on crosslink reactivity, using low- T_g matrices like PDMS or gels swollen with a good solvent facilitates comparison.
- 2. The network topologies for a series of CANs should be as similar as possible. If K_{eq} varies, quantitative comparison requires the application of appropriate theories. ^{68,69}
- 3. In general, amorphous prepolymers with lower dispersity, well-defined junction functionality, and molecular weight below entanglement yield networks that better approximate "ideal" topology.^{65,66} Networks derived from multifunctional monomers, while synthetically expedient, may experience changes in *T*_g, matrix polarity, crosslink density, defect formation, or backbone flexibility when the crosslink is modified in addition to the desired changes in reactivity.
- 4. While most CANs are assembled using the dynamic covalent bond itself, more uniform network topologies may be achieved by embedding the dynamic covalent bond in the strand and curing the network by a rapid, efficient "click"-type reaction. 144 This is particularly true if the dynamic bonds span a wide range of kinetics.

4.3 NETWORKS ARE NOT IDEAL

In permanent networks, it is well understood that even if networks could be prepared using unimolecular prepolymers, per-

fect stoichiometry, and quantitative reactions, the resulting topologies can never be "ideal" because the formation of some fraction of intramolecular linkages (loops) is inevitable. However, the consequences of non-ideality in CANs are only just beginning to be explored. In addition to theories that address the contribution of loops to elasticity⁵⁹ and fracture, 145 theory by Ciarella suggests that loops in vitrimers in fact accelerate network rearrangement by converting elastically-active strands into elastically-inactive (or fractionally-elastically-active) loops that dissipate stress while maintaining crosslink connectivity. 5853 However, experimental studies to date provide only indirect support for this prediction.^{32,55} To confirm and quantify this theory experimentally, studies that count loops in CANs, systematically vary loop fraction in materials with identical dynamic bonds, 146,147 and evaluate the effect on stress relaxation are required.

4.4 TECHNIQUES FOR DIRECT MEASUREMENT IN POLYMER NETWORKS ARE NEEDED

In the studies highlighted here, trends in polymer networks with respect to crosslink structure are almost invariably less well-behaved than the corresponding small-molecule model systems. While the reasons for these discrepancies and strategies to minimize them are discussed above, techniques that enable *direct* measurement of dynamic bond reactivity in the network environment, and particularly under deformation, would offer profound insights to the field. It would be possible to answer questions such as: How do the kinetics and thermodynamics of dynamic bonds in CANs differ from small-molecule model studies? What factors determine these differences? How does deformation affect the dynamic reaction landscape?¹⁴⁸

For dissociative bonds with distinct spectroscopic signatures, solid-state FTIR, Raman, or NMR can be used to quantify the extent of dynamic bond formation.⁴ However, measuring the kinetics of molecular events in materials remains challenging and is rarely performed.^{68,69} Bowman used dielectric (electrochemical impedence) spectroscopy to reveal the timescales of competing dynamic reactions in thioester CANs.^{149,150} This technique benefits from the broad dynamic range relative to oscillatory rheology (10⁻²–10⁹ Hz), but faces similar challenges in assigning relaxation events to molecular processes.

Significant advances in single-particle tracking and superresolution microscopy¹⁵¹ provide time-resolved, nano- to microscale insight into polymerization kinetics^{152–154} and conformations of neat polymer chains.^{155,156} We believe that the development of fluorescent probes that are responsive to dissociative bond formation/breaking¹⁵⁷ or even associative, (quasi)-degenerate bond exchange would allow these optical techniques to be applied to CANs. The ability to map molecular events in time and space, as a function of applied deformations, will illuminate open questions in this field.

Supporting Information

The Supporting Information is available free of charge on the ACS Publications website.

Procedure for extracting Sterimol parameters using DBSTEP and xyz coordinates (PDF)

AUTHOR INFORMATION

Corresponding Author

* jkalow@northwestern.edu

Author Contributions

‡These authors contributed equally.

ACKNOWLEDGMENT

V. Z. and B.K. were supported by the National Institute of General Medical Sciences of the National Institutes of Health under award number R01GM132677. V.Z. was partially supported by the National Institute of Diabetes and Digestive and Kidney Diseases of the National Institutes of Health under award number F30DK129002. J.V.A. was supported by the NSF Center for the Chemistry of Molecularly Optimized Networks (MONET), CHE-2116298. This content is solely the responsibility of the authors and does not necessarily represent the official views of the National Science Foundation or National Institutes of Health. J.A.K. is supported by a Sloan Research Fellowship and a Dreyfus Teacher-Scholar Award.

REFERENCES

- (1) U.S. Synthetic Rubber Program National Historic Chemical Landmark https://www.acs.org/content/acs/en/education/whatischemistry/landmarks/syntheticrubber.html (accessed 2022 07 -28).
- (2) Mäki, J. M.; Sormunen, R.; Lippo, S.; Kaarteenaho-Wiik, R.; Soininen, R.; Myllyharju, J. Lysyl Oxidase Is Essential for Normal Development and Function of the Respiratory System and for the Integrity of Elastic and Collagen Fibers in Various Tissues. *Am. J. Pathol.* **2005**, *167*, 927–936.
- (3) Gregory, D.; Marshall, D. SEM of collagen. https://well-comecollection.org/works/er7vgdus (accessed 2022-11-01).
- (4) Danielsen, S. P. O.; Beech, H. K.; Wang, S.; El-Zaatari, B. M.; Wang, X.; Sapir, L.; Ouchi, T.; Wang, Z.; Johnson, P. N.; Hu, Y.; Lundberg, D. J.; Stoychev, G.; Craig, S. L.; Johnson, J. A.; Kalow, J. A.; Olsen, B. D.; Rubinstein, M. Molecular Characterization of Polymer Networks. *Chem. Rev.* **2021**, *121*, 5042–5092.
- (5) Webber, M. J.; Tibbitt, M. W. Dynamic and Reconfigurable Materials from Reversible Network Interactions. *Nat. Rev. Mater.* **2022**, *7*, 541–556.
- (6) Kloxin, C. J.; Scott, T. F.; Adzima, B. J.; Bowman, C. N. Covalent Adaptable Networks (CANs). *Macromolecules* **2010**, *43*, 2643–2653.
- (7) Zou, W.; Dong, J.; Luo, Y.; Zhao, Q.; Xie, T. Dynamic Covalent Polymer Networks. *Adv. Mater.* **2017**, *29*, 1606100.
- (8) Van Lijsebetten, F.; Debsharma, T.; Winne, J. M.; Du Prez, F. E. A Highly Dynamic Covalent Polymer Network without Creep. *Angew. Chem. Int. Ed.* **2022**.
- (9) Yount, W. C.; Juwarker, H.; Craig, S. L. Orthogonal Control of Dissociation Dynamics Relative to Thermodynamics in a Main-Chain Reversible Polymer. *J. Am. Chem. Soc.* **2003**, *125*, 15302–15303.
- (10) Yount, W. C.; Loveless, D. M.; Craig, S. L. Small-Molecule Dynamics and Mechanisms Underlying the Macroscopic Mechanical Properties of Coordinatively Cross-Linked Polymer Networks. *J. Am. Chem. Soc.* **2005**, *127*, 14488–14496.
- (11) Serpe, M. J.; Craig, S. L. Physical Organic Chemistry of Supramolecular Polymers. *Langmuir* **2007**, *23*, 1626–1634.
- (12) Holten-Andersen, N.; Jaishankar, A.; Harrington, M. J.; Fullenkamp, D. E.; DiMarco, G.; He, L.; McKinley, G. H.; Messersmith, P. B.; Lee, K. Y. C. Metal-Coordination. *J. Mater. Chem. B* **2014**, *2*, 2467–2472.
- (13) Appel, E. A.; Forster, R. A.; Koutsioubas, A.; Toprakcioglu, C.; Scherman, O. A. Activation Energies Control the Macroscopic Properties of Physically Cross-Linked Materials. *Angew. Chem. Int. Ed.* **2014**, *53*, 10038–10043.
- (14) Grindy, S. C.; Learsch, R.; Mozhdehi, D.; Cheng, J.; Barrett, D. G.; Guan, Z.; Messersmith, P. B.; Holten-Andersen, N. Control of

- Hierarchical Polymer Mechanics with Bioinspired Metal-Coordination Dynamics. *Nat. Mater.* **2015**, *14*, 1210–1216.
- (15) Yun Tan, C. S.; Agmon, G.; Liu, J.; Hoogland, D.; Janeček, E.-R.; A. Appel, E.; A. Scherman, O. Distinguishing Relaxation Dynamics in Transiently Crosslinked Polymeric Networks. *Polym. Chem.* **2017**, *8*, 5336–5343.
- (16) Appel, E. A.; del Barrio, J.; Loh, X. J.; Scherman, O. A. Supramolecular Polymeric Hydrogels. *Chem. Soc. Rev.* **2012**, *41*, 6195.
- (17) Voorhaar, L.; Hoogenboom, R. Supramolecular Polymer Networks. *Chem. Soc. Rev.* **2016**, *45*, 4013–4031.
- (18) Webber, M. J.; Appel, E. A.; Meijer, E. W.; Langer, R. Supramolecular Biomaterials. *Nat. Mater.* **2016**, *15*, 13–26.
- (19) Rowan, S. J.; Cantrill, S. J.; Cousins, G. R. L.; Sanders, J. K. M.; Stoddart, J. F. Dynamic Covalent Chemistry. *Angew. Chem. Int. Ed.* **2002**, *41*, 898–952.
- (20) Scheutz, G. M.; Lessard, J. J.; Sims, M. B.; Sumerlin, B. S. Adaptable Crosslinks in Polymeric Materials. *J. Am. Chem. Soc.* **2019**, *141*, 16181–16196.
- (21) De Alwis Watuthanthrige, N.; Chakma, P.; Konkolewicz, D. Designing Dynamic Materials from Dynamic Bonds to Macromolecular Architecture. *Trends Chem.* **2021**, *3*, 231–247.
- (22) Zheng, N.; Xu, Y.; Zhao, Q.; Xie, T. Dynamic Covalent Polymer Networks. *Chem. Rev.* **2021**, *121*, 1716–1745.
- (23) Elling, B. R.; Dichtel, W. R. Reprocessable Cross-Linked Polymer Networks. *ACS Cent. Sci.* **2020**, *6*, 1488–1496.
- (24) Podgórski, M.; Fairbanks, B. D.; Kirkpatrick, B. E.; McBride, M.; Martinez, A.; Dobson, A.; Bongiardina, N. J.; Bowman, C. N. Toward Stimuli-Responsive Dynamic Thermosets through Continuous Development and Improvements in Covalent Adaptable Networks (CANs). *Adv. Mater.* **2020**, *32*, 1906876.
- (25) Montarnal, D.; Capelot, M.; Tournilhac, F.; Leibler, L. Silica-Like Malleable Materials from Permanent Organic Networks. *Science* **2011**, *334*, 965–968.
- (26) Denissen, W.; M. Winne, J.; Prez, F. E. D. Vitrimers. *Chem. Sci.* **2016**, *7*, 30–38.
- (27) Guerre, M.; Taplan, C.; Winne, J. M.; Du Prez, F. E. Vitrimers. *Chem. Sci.* **2020**, *11*, 4855–4870.
- (28) Porath, L.; Soman, B.; Jing, B. B.; Evans, C. M. Vitrimers. *ACS Macro Lett.* **2022**, *11*, 475–483.
- (29) Breuillac, A.; Kassalias, A.; Nicolaÿ, R. Polybutadiene Vitrimers Based on Dioxaborolane Chemistry and Dual Networks with Static and Dynamic Cross-Links. *Macromolecules* **2019**, *52*, 7102–7113.
- (30) Hajj, R.; Duval, A.; Dhers, S.; Avérous, L. Network Design to Control Polyimine Vitrimer Properties. *Macromolecules* **2020**, *53*, 3796–3805.
- (31) Schoustra, S. K.; Dijksman, J. A.; Zuilhof, H.; Smulders, M. M. J. Molecular Control over Vitrimer-like Mechanics Tuneable Dynamic Motifs Based on the Hammett Equation in Polyimine Materials. *Chem. Sci.* **2021**, *12*, 293–302.
- (32) Ishibashi, J. S. A.; Pierce, I. C.; Chang, A. B.; Zografos, A.; El-Zaatari, B. M.; Fang, Y.; Weigand, S. J.; Bates, F. S.; Kalow, J. A. Mechanical and Structural Consequences of Associative Dynamic Cross-Linking in Acrylic Diblock Copolymers. *Macromolecules* **2021**, *54*, 3972–3986.
- (33) Winne, J. M.; Leibler, L.; Du Prez, F. E. Dynamic Covalent Chemistry in Polymer Networks. *Polym. Chem.* **2019**, *10*, 6091–6108.
- (34) Ciaccia, M.; Di Stefano, S. Mechanisms of Imine Exchange Reactions in Organic Solvents. *Org. Biomol. Chem.* **2015**, *13*, 646–654.
- (35) Iwatsuki, S.; Nakajima, S.; Inamo, M.; Takagi, H. D.; Ishihara, K. Which Is Reactive in Alkaline Solution, Boronate Ion or Boronic Acid? *Inorg. Chem.* **2007**, *46*, 354–356.
- (36) Martínez-Aguirre, M. A.; Villamil-Ramos, R.; Guerrero-Alvarez, J. A.; Yatsimirsky, A. K. Substituent Effects and PH Profiles for Stability Constants of Arylboronic Acid Diol Esters. *J. Org. Chem.* **2013**, *78*, 4674–4684.
- (37) Furikado, Y.; Nagahata, T.; Okamoto, T.; Sugaya, T.; Iwatsuki, S.; Inamo, M.; Takagi, H. D.; Odani, A.; Ishihara, K. Universal Reaction Mechanism of Boronic Acids with Diols in Aqueous Solution. *Chem. Eur. J.* **2014**, *20*, 13194–13202.

- (38) Marco-Dufort, B.; Tibbitt, M. W. Design of Moldable Hydrogels for Biomedical Applications Using Dynamic Covalent Boronic Esters. *Mater. Today Chem.* **2019**, *12*, 16–33.
- (39) Röttger, M.; Domenech, T.; van der Weegen, R.; Breuillac, A.; Nicolaÿ, R.; Leibler, L. High-Performance Vitrimers from Commodity Thermoplastics through Dioxaborolane Metathesis. *Science* **2017**, *356*, 62–65.
- (40) Obadia, M. M.; Mudraboyina, B. P.; Serghei, A.; Montarnal, D.; Drockenmuller, E. Reprocessing and Recycling of Highly Cross-Linked Ion-Conducting Networks through Transalkylation Exchanges of C–N Bonds. *J. Am. Chem. Soc.* **2015**, *137*, 6078–6083.
- (41) Obadia, M. M.; Jourdain, A.; Cassagnau, P.; Montarnal, D.; Drockenmuller, E. Tuning the Viscosity Profile of Ionic Vitrimers Incorporating 1,2,3-Triazolium Cross-Links. *Adv. Funct. Mater.* **2017**, 27, 1703258.
- (42) Hendriks, B.; Waelkens, J.; Winne, J. M.; Du Prez, F. E. Poly(Thioether) Vitrimers via Transalkylation of Trialkylsulfonium Salts. *ACS Macro Lett.* **2017**, *6*, 930–934.
- (43) Chakma, P.; Morley, C. N.; Sparks, J. L.; Konkolewicz, D. Exploring How Vitrimer-like Properties Can Be Achieved from Dissociative Exchange in Anilinium Salts. *Macromolecules* **2020**, *53*, 1233–1244
- (44) Tanaka, F.; Edwards, S. F. Viscoelastic Properties of Physically Crosslinked Networks. 1. Transient Network Theory. *Macromolecules* **1992**, *25*, 1516–1523.
- (45) Cates, M. E. Stress Relaxation and Chemical Kinetics in Pairwise Associating Polymers. *Macromolecules* **1988**, *21*, 256–259.
- (46) Moacanin, J.; Aklonis, J. J. Viscoelastic Behavior of Polymers Undergoing Crosslinking Reactions. *J. Polym. Sci. Part C Polym. Symp.* **1971**, *35*, 71–76.
- (47) Fricker, H. On the Theory of Stress Relaxation by Cross-Link Reorganization. *Proc. R. Soc. Lond. Math. Phys. Sci.* **1973**, *335*, 289–300.
- (48) Green, M. S.; Tobolsky, A. V. A New Approach to the Theory of Relaxing Polymeric Media. *J. Chem. Phys.* **1946**, *14*, 80–92.
- (49) Leibler, L.; Rubinstein, M.; Colby, R. H. Dynamics of Reversible Networks. *Macromolecules* **1991**, *24*, 4701–4707.
- (50) Rubinstein, M.; Semenov, A. N. Dynamics of Entangled Solutions of Associating Polymers. *Macromolecules* **2001**, *34*, 1058–1068
- (51) Long, R.; Qi, H. J.; Dunn, M. L. Modeling the Mechanics of Covalently Adaptable Polymer Networks with Temperature-Dependent Bond Exchange Reactions. *Soft Matter* **2013**, *9*, 4083–4096.
- (52) Meng, F.; Pritchard, R. H.; Terentjev, E. M. Stress Relaxation, Dynamics, and Plasticity of Transient Polymer Networks. *Macromolecules* **2016**, *49*, 2843–2852.
- (53) Ciarella, S.; Sciortino, F.; Ellenbroek, W. G. Dynamics of Vitrimers: Defects as a Highway to Stress Relaxation. *Phys. Rev. Lett.* **2018**, *121*, 058003.
- (54) Meng, F.; Saed, M. O.; Terentjev, E. M. Elasticity and Relaxation in Full and Partial Vitrimer Networks. *Macromolecules* **2019**, *52*, 7423–7429.
- (55) Ricarte, R. G.; Tournilhac, F.; Cloître, M.; Leibler, L. Linear Viscoelasticity and Flow of Self-Assembled Vitrimers. *Macromolecules* **2020**, *53*, 1852–1866.
- (56) Perego, A.; Khabaz, F. Effect of Bond Exchange Rate on Dynamics and Mechanics of Vitrimers. *J. Polym. Sci.* **2021**, *59*, 2590–2602.
- (57) Rubinstein, M.; Colby, R. H. *Polymer Physics*; Oxford University Press: Oxford; New York, 2003.
- (58) Flory, P. J. Molecular Theory of Rubber Elasticity. *Polym. J.* **1985**, *17*, 1–12.
- (59) Zhong, M.; Wang, R.; Kawamoto, K.; Olsen, B. D.; Johnson, J. A. Quantifying the Impact of Molecular Defects on Polymer Network Elasticity. *Science* **2016**, *353*, 1264–1268.
- (60) Wang, R.; Alexander-Katz, A.; Johnson, J. A.; Olsen, B. D. Universal Cyclic Topology in Polymer Networks. *Phys. Rev. Lett.* **2016**, *116*, 188302.
- (61) Zhou, H.; Woo, J.; Cok, A. M.; Wang, M.; Olsen, B. D.; Johnson, J. A. Counting Primary Loops in Polymer Gels. *Proc. Natl. Acad. Sci.* **2012**, *109*, 19119–19124.

- (62) Zhou, H.; Schön, E.-M.; Wang, M.; Glassman, M. J.; Liu, J.; Zhong, M.; Díaz Díaz, D.; Olsen, B. D.; Johnson, J. A. Crossover Experiments Applied to Network Formation Reactions. *J. Am. Chem. Soc.* **2014**, *136*, 9464–9470.
- (63) Kawamoto, K.; Zhong, M.; Wang, R.; Olsen, B. D.; Johnson, J. A. Loops versus Branch Functionality in Model Click Hydrogels. *Macromolecules* **2015**, *48*, 8980–8988.
- (64) Adzima, B. J.; Aguirre, H. A.; Kloxin, C. J.; Scott, T. F.; Bowman, C. N. Rheological and Chemical Analysis of Reverse Gelation in a Covalently Cross-Linked Diels-Alder Polymer Network. *Macromolecules* **2008**, *41*, 9112–9117.
- (65) Parada, G. A.; Zhao, X. Ideal Reversible Polymer Networks. *Soft Matter* **2018**, *14*, 5186–5196.
- (66) Marco-Dufort, B.; Iten, R.; Tibbitt, M. W. Linking Molecular Behavior to Macroscopic Properties in Ideal Dynamic Covalent Networks. *J. Am. Chem. Soc.* **2020**, *142*, 15371–15385.
- (67) Rubinstein, M.; Semenov, A. N. Thermoreversible Gelation in Solutions of Associating Polymers. 2. Linear Dynamics. *Macromolecules* **1998**, *31*, 1386–1397.
- (68) Sheridan, R. J.; Bowman, C. N. A Simple Relationship Relating Linear Viscoelastic Properties and Chemical Structure in a Model Diels–Alder Polymer Network. *Macromolecules* **2012**, *45*, 7634–7641.
- (69) Kuang, X.; Liu, G.; Dong, X.; Wang, D. Correlation between Stress Relaxation Dynamics and Thermochemistry for Covalent Adaptive Networks Polymers. *Mater. Chem. Front.* **2017**, *1*, 111–118.
- (70) Katashima, T.; Kudo, R.; Naito, M.; Nagatoishi, S.; Miyata, K.; Chung, U.; Tsumoto, K.; Sakai, T. Experimental Comparison of Bond Lifetime and Viscoelastic Relaxation in Transient Networks with Well-Controlled Structures. *ACS Macro Lett.* **2022**, *11*, 753–759.
- (71) Stukalin, E. B.; Cai, L.-H.; Kumar, N. A.; Leibler, L.; Rubinstein, M. Self-Healing of Unentangled Polymer Networks with Reversible Bonds. *Macromolecules* **2013**, *46*, 7525–7541.
- (72) He, C.; Shi, S.; Wu, X.; Russell, T. P.; Wang, D. Atomic Force Microscopy Nanomechanical Mapping Visualizes Interfacial Broadening between Networks Due to Chemical Exchange Reactions. *J. Am. Chem. Soc.* **2018**, *140*, 6793–6796.
- (73) Lagron, A. B.; El-Zaatari, B. M.; Hamachi, L. S. Characterization Techniques to Assess Recyclability in Dynamic Polymer Networks. *Front. Mater.* **2022**, *9*, 915296.
- (74) Zhang, L.; Rowan, S. J. Effect of Sterics and Degree of Cross-Linking on the Mechanical Properties of Dynamic Poly(Alkylurea–Urethane) Networks. *Macromolecules* **2017**, *50*, 5051–5060.
- (75) Herbert, K. M.; Getty, P. T.; Dolinski, N. D.; Hertzog, J. E.; Jong, D. de; Lettow, J. H.; Romulus, J.; Onorato, J. W.; Foster, E. M.; Rowan, S. J. Dynamic Reaction-Induced Phase Separation in Tunable, Adaptive Covalent Networks. *Chem. Sci.* **2020**, *11*, 5028–5036.
- (76) Majumdar, S.; Mezari, B.; Zhang, H.; van Aart, J.; van Benthem, R. A. T. M.; Heuts, J. P. A.; Sijbesma, R. P. Efficient Exchange in a Bioinspired Dynamic Covalent Polymer Network via a Cyclic Phosphate Triester Intermediate. *Macromolecules* **2021**, *54*, 7955–7962.
- (77) Hu, W.-H.; Chen, T.-T.; Tamura, R.; Terayama, K.; Wang, S.; Watanabe, I.; Naito, M. Topological Alternation from Structurally Adaptable to Mechanically Stable Crosslinked Polymer. *Sci. Technol. Adv. Mater.* **2022**, *23*, 66–75.
- (78) Van Lijsebetten, F.; De Bruycker, K.; Van Ruymbeke, E.; Winne, J. M.; Du Prez, F. E. Characterising Different Molecular Landscapes in Dynamic Covalent Networks. *Chem. Sci.* **2022**, 10.1039.D2SC05528G.
- (79) Guerre, M.; Taplan, C.; Nicolaÿ, R.; Winne, J. M.; Du Prez, F. E. Fluorinated Vitrimer Elastomers with a Dual Temperature Response. *J. Am. Chem. Soc.* **2018**, *140*, 13272–13284.
- (80) Porath, L. E.; Evans, C. M. Importance of Broad Temperature Windows and Multiple Rheological Approaches for Probing Viscoelasticity and Entropic Elasticity in Vitrimers. *Macromolecules* **2021**, *54*, 4782–4791.
- (81) Ricarte, R. G.; Shanbhag, S. Unentangled Vitrimer Melts. *Macromolecules* **2021**, *54*, 3304–3320.

- (82) Wang, S.; Ma, S.; Li, Q.; Yuan, W.; Wang, B.; Zhu, J. Robust, Fire-Safe, Monomer-Recovery, Highly Malleable Thermosets from Renewable Bioresources. *Macromolecules* **2018**, *51*, 8001–8012.
- (83) Fortman, D. J.; Brutman, J. P.; Hillmyer, M. A.; Dichtel, W. R. Structural Effects on the Reprocessability and Stress Relaxation of Crosslinked Polyhydroxyurethanes. *J. Appl. Polym. Sci.* **2017**, *134*, 44984
- (84) Spiesschaert, Y.; Taplan, C.; Stricker, L.; Guerre, M.; Winne, J. M.; Prez, F. E. D. Influence of the Polymer Matrix on the Viscoelastic Behaviour of Vitrimers. *Polym. Chem.* **2020**, *11*, 5377–5385.
- (85) He, C.; Christensen, P. R.; Seguin, T. J.; Dailing, E. A.; Wood, B. M.; Walde, R. K.; Persson, K. A.; Russell, T. P.; Helms, B. A. Conformational Entropy as a Means to Control the Behavior of Poly(Diketoenamine) Vitrimers In and Out of Equilibrium. *Angew. Chem. Int. Ed.* **2020**, *59*, 735–739.
- (86) Kang, B.; Kalow, J. A. Internal and External Catalysis in Boronic Ester Networks. *ACS Macro Lett.* **2022**, *11*, 394–401.
- (87) Suzuki, Y.; Kusuyama, D.; Sugaya, T.; Iwatsuki, S.; Inamo, M.; Takagi, H. D.; Ishihara, K. Reactivity of Boronic Acids toward Catechols in Aqueous Solution. *J. Org. Chem.* **2020**, *85*, 5255–5264.
- (88) Santiago, C. B.; Guo, J.-Y.; Sigman, M. S. Predictive and Mechanistic Multivariate Linear Regression Models for Reaction Development. *Chem. Sci.* **2018**, *9*, 2398–2412.
- (89) Zahrt, A. F.; Athavale, S. V.; Denmark, S. E. Quantitative Structure–Selectivity Relationships in Enantioselective Catalysis. *Chem. Rev.* **2020**, *120*, 1620–1689.
- (90) Williams, W. L.; Zeng, L.; Gensch, T.; Sigman, M. S.; Doyle, A. G.; Anslyn, E. V. The Evolution of Data-Driven Modeling in Organic Chemistry. *ACS Cent. Sci.* **2021**, *7*, 1622–1637.
- (91) Harper, K. C.; Sigman, M. S. Using Physical Organic Parameters To Correlate Asymmetric Catalyst Performance. *J. Org. Chem.* **2013**, *78*, 2813–2818.
- (92) Hansch, Corwin.; Leo, A.; Taft, R. W. A Survey of Hammett Substituent Constants and Resonance and Field Parameters. *Chem. Rev.* **1991**, *91*, 165–195.
- (93) Van Herck, N.; Maes, D.; Unal, K.; Guerre, M.; Winne, J. M.; Du Prez, F. E. Covalent Adaptable Networks with Tunable Exchange Rates Based on Reversible Thiol—Yne Cross-Linking. *Angew. Chem.* **2020**, *132*, 3637–3646.
- (94) Rohatgi, A. WebPlotDigitizer: version 4.6 https://apps.automeris.io/wpd/ (accessed 2022-07-31).
- (95) FitzSimons, T. M.; Oentoro, F.; Shanbhag, T. V.; Anslyn, E. V.; Rosales, A. M. Preferential Control of Forward Reaction Kinetics in Hydrogels Crosslinked with Reversible Conjugate Additions. *Macromolecules* **2020**, *53*, 3738–3746.
- (96) Gablier, A.; O. Saed, M.; M. Terentjev, E. Rates of Transesterification in Epoxy–Thiol Vitrimers. *Soft Matter* **2020**, *16*, 5195–5202
- (97) Ying, H.; Zhang, Y.; Cheng, J. Dynamic Urea Bond for the Design of Reversible and Self-Healing Polymers. *Nat. Commun.* **2014**, *5*, 3218.
- (98) Zhang, Y.; Ying, H.; Hart, K. R.; Wu, Y.; Hsu, A. J.; Coppola, A. M.; Kim, T. A.; Yang, K.; Sottos, N. R.; White, S. R.; Cheng, J. Malleable and Recyclable Poly(Urea-Urethane) Thermosets Bearing Hindered Urea Bonds. *Adv. Mater.* **2016**, *28*, 7646–7651.
- (99) Ying, H.; Cheng, J. Hydrolyzable Polyureas Bearing Hindered Urea Bonds. J. Am. Chem. Soc. 2014, 136, 16974–16977.
- (100) Hutchby, M.; Houlden, C. E.; Ford, J. G.; Tyler, S. N. G.; Gagné, M. R.; Lloyd-Jones, G. C.; Booker-Milburn, K. I. Hindered Ureas as Masked Isocyanates. *Angew. Chem. Int. Ed.* **2009**, *48*, 8721–8724
- (101) Luchini, G.; Patterson, T.; Paton, R. S. DBSTEP: DFT Based Steric Parameters. 2022, 10.5281/zenodo.4702097.
- (102) Brethomé, A. V.; Fletcher, S. P.; Paton, R. S. Conformational Effects on Physical-Organic Descriptors. *ACS Catal.* **2019**, *9*, 2313–2323.
- (103) Soman, B.; Evans, C. M. Effect of Precise Linker Length, Bond Density, and Broad Temperature Window on the Rheological Properties of Ethylene Vitrimers. *Soft Matter* **2021**, *17*, 3569–3577.

- (104) Guimard, N. K.; Ho, J.; Brandt, J.; Lin, C. Y.; Namazian, M.; Mueller, J. O.; Oehlenschlaeger, K. K.; Hilf, S.; Lederer, A.; Schmidt, F. G.; Coote, M. L.; Barner-Kowollik, C. Harnessing Entropy to Direct the Bonding/Debonding of Polymer Systems Based on Reversible Chemistry. *Chem. Sci.* **2013**, *4*, 2752–2759.
- (105) Capon, B. Neighbouring Group Participation. *Q. Rev. Chem. Soc.* **1964**, *18*, 45–111.
- (106) Schramm, V. L. Enzymatic Transition States and Transition State Analog Design. *Annu. Rev. Biochem.* **1998**, *67*, 693–720.
- (107) Lijsebetten, F. V.; Holloway, J. O.; Winne, J. M.; Prez, F. E. D. Internal Catalysis for Dynamic Covalent Chemistry Applications and Polymer Science. *Chem. Soc. Rev.* **2020**, *49*, 8425–8438.
- (108) Cuminet, F.; Caillol, S.; Dantras, É.; Leclerc, É.; Ladmiral, V. Neighboring Group Participation and Internal Catalysis Effects on Exchangeable Covalent Bonds. *Macromolecules* **2021**, *54*, 3927–3961.
- (109) Delahaye, M.; Winne, J. M.; Du Prez, F. E. Internal Catalysis in Covalent Adaptable Networks. *J. Am. Chem. Soc.* **2019**, *141*, 15277–15287.
- (110) Wulff, G.; Lauer, M.; Böhnke, H. Rapid Proton Transfer as Cause of an Unusually Large Neighboring Group Effect. *Angew. Chem. Int. Ed. Engl.* **1984**, *23*, 741–742.
- (111) Cromwell, O. R.; Chung, J.; Guan, Z. Malleable and Self-Healing Covalent Polymer Networks through Tunable Dynamic Boronic Ester Bonds. *J. Am. Chem. Soc.* **2015**, *137*, 6492–6495.
- (112) Nishimura, Y.; Chung, J.; Muradyan, H.; Guan, Z. Silyl Ether as a Robust and Thermally Stable Dynamic Covalent Motif for Malleable Polymer Design. *J. Am. Chem. Soc.* **2017**, *139*, 14881–14884.
- (113) Collins, B. E.; Metola, P.; Anslyn, E. V. On the Rate of Boronate Ester Formation in Ortho-Aminomethyl-Functionalised Phenyl Boronic Acids. *Supramol. Chem.* **2013**, *25*, 79–86.
- (114) Sun, X.; Chapin, B. M.; Metola, P.; Collins, B.; Wang, B.; James, T. D.; Anslyn, E. V. The Mechanisms of Boronate Ester Formation and Fluorescent Turn-on in Ortho-Aminomethylphenylboronic Acids. *Nat. Chem.* **2019**, *11*, 768–778.
- (115) Fortman, D. J.; Brutman, J. P.; Cramer, C. J.; Hillmyer, M. A.; Dichtel, W. R. Mechanically Activated, Catalyst-Free Polyhydroxyurethane Vitrimers. *J. Am. Chem. Soc.* **2015**, *137*, 14019–14022.
- (116) Hernández, A.; Houck, H. A.; Elizalde, F.; Guerre, M.; Sardon, H.; Du Prez, F. E. Internal Catalysis on the Opposite Side of the Fence in Non-Isocyanate Polyurethane Covalent Adaptable Networks. *Eur. Polym. J.* **2022**, *168*, 111100.
- (117) Ishibashi, J. S. A.; Kalow, J. A. Vitrimeric Silicone Elastomers Enabled by Dynamic Meldrum's Acid-Derived Cross-Links. *ACS Macro Lett.* **2018**, *7*, 482–486.
- (118) El-Zaatari, B. M.; Ishibashi, J. S. A.; Kalow, J. A. Cross-Linker Control of Vitrimer Flow. *Polym. Chem.* 2020, 11, 5339–5345.
- (119) Truong, V. X.; Barner-Kowollik, C. Photodynamic Covalent Bonds Regulated by Visible Light for Soft Matter Materials. *Trends Chem.* **2022**, *4*, 291–304.
- (120) Asadirad, A. M.; Boutault, S.; Erno, Z.; Branda, N. R. Controlling a Polymer Adhesive Using Light and a Molecular Switch. *J. Am. Chem. Soc.* **2014**, *136*, 3024–3027.
- (121) Fuhrmann, A.; Göstl, R.; Wendt, R.; Kötteritzsch, J.; Hager, M. D.; Schubert, U. S.; Brademann-Jock, K.; Thünemann, A. F.; Nöchel, U.; Behl, M.; Hecht, S. Conditional Repair by Locally Switching the Thermal Healing Capability of Dynamic Covalent Polymers with Light. *Nat. Commun.* **2016**, *7*, 13623.
- (122) Truong, V. X.; Li, F.; Ercole, F.; Forsythe, J. S. Wavelength-Selective Coupling and Decoupling of Polymer Chains via Reversible [2 + 2] Photocycloaddition of Styrylpyrene for Construction of Cytocompatible Photodynamic Hydrogels. *ACS Macro Lett.* **2018**, *7*, 464–469.
- (123) Froimowicz, P.; Frey, H.; Landfester, K. Towards the Generation of Self-Healing Materials by Means of a Reversible Photo-Induced Approach. *Macromol. Rapid Commun.* **2011**, *32*, 468–473.
- (124) Kabb, C. P.; O'Bryan, C. S.; Deng, C. C.; Angelini, T. E.; Sumerlin, B. S. Photoreversible Covalent Hydrogels for Soft-Matter Additive Manufacturing. *ACS Appl. Mater. Interfaces* **2018**, *10*, 16793–16801.

- (125) Kathan, M.; Kovaříček, P.; Jurissek, C.; Senf, A.; Dallmann, A.; Thünemann, A. F.; Hecht, S. Control of Imine Exchange Kinetics with Photoswitches to Modulate Self-Healing in Polysiloxane Networks by Light Illumination. *Angew. Chem. Int. Ed.* **2016**, *55*, 13882–13886.
- (126) Accardo, J. V.; Kalow, J. A. Reversibly Tuning Hydrogel Stiffness through Photocontrolled Dynamic Covalent Crosslinks. *Chem. Sci.* **2018**, *9*, 5987–5993.
- (127) Accardo, J. V.; McClure, E. R.; Mosquera, M. A.; Kalow, J. A. Using Visible Light to Tune Boronic Acid–Ester Equilibria. *J. Am. Chem. Soc.* **2020**, *142*, 19969–19979.
- (128) Barsoum, D. N.; Kirinda, V. C.; Kang, B.; Kalow, J. A. Remote-Controlled Exchange Rates by Photoswitchable Internal Catalysis of Dynamic Covalent Bonds. *J. Am. Chem. Soc.* **2022**, *144*, 10168–10173.
- (129) Worrell, B. T.; McBride, M. K.; Lyon, G. B.; Cox, L. M.; Wang, C.; Mavila, S.; Lim, C.-H.; Coley, H. M.; Musgrave, C. B.; Ding, Y.; Bowman, C. N. Bistable and Photoswitchable States of Matter. *Nat. Commun.* **2018**, *9*, 2804.
- (130) Scott, T. F.; Schneider, A. D.; Cook, W. D.; Bowman, C. N. Photoinduced Plasticity in Cross-Linked Polymers. *Science* **2005**, *308*, 1615–1617.
- (131) Kloxin, C. J.; Scott, T. F.; Park, H. Y.; Bowman, C. N. Mechanophotopatterning on a Photoresponsive Elastomer. *Adv. Mater.* **2011**, *23*, 1977–1981.
- (132) Yavitt, F. M.; Brown, T. E.; Hushka, E. A.; Brown, M. E.; Gjorevski, N.; Dempsey, P. J.; Lutolf, M. P.; Anseth, K. S. The Effect of Thiol Structure on Allyl Sulfide Photodegradable Hydrogels and Their Application as a Degradable Scaffold for Organoid Passaging. *Adv. Mater.* **2020**, *32*, 1905366.
- (133) Fairbanks, B. D.; Singh, S. P.; Bowman, C. N.; Anseth, K. S. Photodegradable, Photoadaptable Hydrogels via Radical-Mediated Disulfide Fragmentation Reaction. *Macromolecules* **2011**, *44*, 2444–2450.
- (134) Lemieux, V.; Gauthier, S.; Branda, N. R. Selective and Sequential Photorelease Using Molecular Switches. *Angew. Chem. Int. Ed.* **2006**, *45*, 6820–6824.
- (135) Göstl, R.; Hecht, S. Controlling Covalent Connection and Disconnection with Light. *Angew. Chem. Int. Ed.* **2014**, *53*, 8784–8787.
- (136) Brooks, W. L. A.; Sumerlin, B. S. Synthesis and Applications of Boronic Acid-Containing Polymers. *Chem. Rev.* **2016**, *116*, 1375–1397.
- (137) Bandara, H. M. D.; Burdette, S. C. Photoisomerization in Different Classes of Azobenzene. *Chem. Soc. Rev.* **2012**, *41*, 1809–1825.
- (138) Accardo, J. V.; Kalow, J. A. Reversibly Tuning Hydrogel Stiffness through Photocontrolled Dynamic Covalent Crosslinks. *Chem. Sci.* **2018**, *9*, 5987–5993.
- (139) Li, J.; Nagamani, C.; Moore, J. S. Polymer Mechanochemistry. Acc. Chem. Res. 2015, 48, 2181–2190.
- (140) Du, M.; Houck, H. A.; Yin, Q.; Xu, Y.; Huang, Y.; Lan, Y.; Yang, L.; Du Prez, F. E.; Chang, G. Force–Reversible Chemical Reaction at Ambient Temperature for Designing Toughened Dynamic Covalent Polymer Networks. *Nat. Commun.* **2022**, *13*, 3231.
- (141) Schoustra, S. K.; Groeneveld, T.; Smulders, M. M. J. The Effect of Polarity on the Molecular Exchange Dynamics in Imine-Based Covalent Adaptable Networks. *Polym. Chem.* **2021**, *12*, 1635–1642.
- (142) Ricarte, R. G.; Tournilhac, F.; Leibler, L. Phase Separation and Self-Assembly in Vitrimers. *Macromolecules* **2019**, *52*, 432–443.
- (143) Lessard, J. J.; Scheutz, G. M.; Sung, S. H.; Lantz, K. A.; Epps, T. H.; Sumerlin, B. S. Block Copolymer Vitrimers. *J. Am. Chem. Soc.* **2020**, *142*, 283–289.
- (144) Brown, T. E.; Carberry, B. J.; Worrel, B. T.; Dudaryeva, O. Y.; McBride, M. K.; Bowman, C. N.; Anseth, K. S. Photopolymerized Dynamic Hydrogels with Tunable Viscoelastic Properties through Thioester Exchange. *Biomaterials* **2018**, *178*, 496–503.
- (145) Arora, A.; Lin, T.-S.; Beech, H. K.; Mochigase, H.; Wang, R.; Olsen, B. D. Fracture of Polymer Networks Containing Topological Defects. *Macromolecules* **2020**, *53*, 7346–7355.

- (146) Gu, Y.; Kawamoto, K.; Zhong, M.; Chen, M.; Hore, M. J. A.; Jordan, A. M.; Korley, L. T. J.; Olsen, B. D.; Johnson, J. A. Semibatch Monomer Addition as a General Method to Tune and Enhance the Mechanics of Polymer Networks via Loop-Defect Control. *Proc. Natl. Acad. Sci.* **2017**, *114*, 4875–4880.
- (147) Wang, J.; Wang, R.; Gu, Y.; Sourakov, A.; Olsen, B. D.; Johnson, J. A. Counting Loops in Sidechain-Crosslinked Polymers from Elastic Solids to Single-Chain Nanoparticles. *Chem. Sci.* **2019**, *10*, 5332–5337.
- (148) Liu, Y.; Holm, S.; Meisner, J.; Jia, Y.; Wu, Q.; Woods, T. J.; Martinez, T. J.; Moore, J. S. Flyby Reaction Trajectories. *Science* **2021**, *373*, 208–212.
- (149) Podgórski, M.; Spurgin, N.; Mavila, S.; Bowman, C. N. Mixed Mechanisms of Bond Exchange in Covalent Adaptable Networks. *Polym. Chem.* **2020**, *11*, 5365–5376.
- (150) Bongiardina, N. J.; Long, K. F.; Podgórski, M.; Bowman, C. N. Substituted Thiols in Dynamic Thiol–Thioester Reactions. *Macromolecules* **2021**, *54*, 8341–8351.

- (151) Chapman, D. V.; Du, H.; Lee, W. Y.; Wiesner, U. B. Optical Super-Resolution Microscopy in Polymer Science. *Prog. Polym. Sci.* **2020**, *111*, 101312.
- (152) Eivgi, O.; Blum, S. A. Real-Time Polymer Viscosity–Catalytic Activity Relationships on the Microscale. *J. Am. Chem. Soc.* **2022**, *144*, 13574–13585.
- (153) Saluga, S. J.; Dibble, D. J.; Blum, S. A. Superresolved Motions of Single Molecular Catalysts during Polymerization Show Wide Distributions. *J. Am. Chem. Soc.* **2022**, *144*, 10591–10598.
- (154) Yu, D.; Garcia, A.; Blum, S. A.; Welsher, K. D. Growth Kinetics of Single Polymer Particles in Solution via Active-Feedback 3D Tracking. *J. Am. Chem. Soc.* **2022**, *144*, 14698–14705.
- (155) Chan, J. M.; Kordon, A. C.; Zhang, R.; Wang, M. Direct Visualization of Bottlebrush Polymer Conformations in the Solid State. *Proc. Natl. Acad. Sci.* **2021**, *118*, e2109534118.
- (156) Chan, J. M.; Wang, M. Visualizing the Orientation of Single Polymers Induced by Spin-Coating. *Nano Lett.* **2022**, *22*, 5891–5897.
- (157) Feng, X.; Wu, T.; Sun, X.; Qian, X. "Indanonalkene" Photoluminescence Platform. J. Am. Chem. Soc. 2021, 143, 21622–21629.

